Pontifícia Universidade Católica
do Rio de Janeiro

Mateus Aguiar Rodrigues de Lima

Controlled release of the inner content of gellan gum microcapsules using temperature as the trigger mechanism

Dissertação de Mestrado

Dissertation presented to the Programa de Pós-Graduação em Engenharia Mecânica of PUC-Rio in partial fulfillment of the requirements for the degree of Mestre em Engenharia Mecânica.

Advisor : Prof. Márcio da Silveira Carvalho
Co-advisor: Dr. Jorge Antonio Avendaño Benavides

Rio de Janeiro
June 2022

Pontifícia Universidade Católica
do Rio de Janeiro

Mateus Aguiar Rodrigues de Lima

Controlled release of the inner content of gellan gum microcapsules using temperature as the trigger mechanism

Dissertation presented to the Programa de Pós-Graduação em Engenharia Mecânica of PUC-Rio in partial fulfillment of the requirements for the degree of Mestre em Engenharia Mecânica. Approved by the Examination Committee.

Prof. Márcio da Silveira Carvalho
Advisor
Departamento de Engenharia Mecânica – PUC-Rio

Dr. Jorge Antonio Avendaño Benavides
Co-advisor
Laboratório de Microhidrodinâmica e Escoamento em Meios Porosos (LMMP) – PUC-Rio

Prof. Mariano Michelon
Escola de Química e Alimentos – FURG

Prof. Luis Fernando Alzuguir Azevedo
Departamento de Engenharia Mecânica – PUC-Rio

Dr. Felipe Pereira Fleming
Cenpes – Petrobras

Rio de Janeiro, June the 24th, 2022

Mateus Aguiar Rodrigues de Lima

Bachelor in Mechanical Engineering by Pontifícia Universidade Católica do Rio de Janeiro (PUC-RJ)- 2019.

Bibliographic data

Lima, Mateus Aguiar Rodrigues de

Controlled release of the inner content of gellan gum microcapsules using temperature as the trigger mechanism / Mateus Aguiar Rodrigues de Lima; advisor: Márcio da Silveira Carvalho; co-advisor: Jorge Antonio Avendaño Benavides. - 2022.

91 f.: il. color. ; 30 cm

Dissertação (mestrado) - Pontifícia Universidade Católica do Rio de Janeiro, Departamento de Engenharia Mecânica, 2022.

Inclui bibliografia

1. Engenharia Mecânica – Teses. 2. Microcápsulas. 3. Liberação controlada. 4. Goma gelana. 5. Temperatura. I. Carvalho, Márcio da Silveira. II. Benavides, Jorge Antonio Avendaño. III. Pontifícia Universidade Católica do Rio de Janeiro. Department of Engenharia Mecânica. IV. Título.

CDD: 621

To God and my family for their love.

Acknowledgments

Above all, I thank God for his infinite and unconditional love.

I would like to demonstrate my infinite gratitude for my wonderful parents Eliane and Gilberto. For all their sacrifices made for me and my sister, for their immense friendship and love.

To my sister, Gabriela, for her constant smiles that make my life smooth and pleasurable. Thank you for always advising, guiding and embracing me always.

To my cousin, Marcio, for all the laughs, stories, victories, defeats that life has given us. Thank you so much for always being by my side.

To all my teachers from PUC-RJ who supported me through rough times

To my advisor, Prof. Marcio Carvalho and my co-adviser Jorge for all the conversations we've had over the years. Thank you so much for all the discussions, trust, encouragement, ideas, for taking me out of my comfort zone.

To my friends, and now brothers, Nicholas Ribeiro and Renan Mury that PUC-RJ gave me. Thank you for your kindness, encouragement, jokes, for listening to all my complaints and for never giving up on me.

To Felicle, Leo, Amanda, Raphael, Bruna, Vinicius, Thiago, Sergio, Paulo, Clarice, Alandmara, Andrea, Jesus, Nicolle, Ademir, Talita, Anthony, Lisbeth for the patience, knowledge, wisdom and for making the days in the laboratory lighter.

To my friends Rodrigo Castelo, Vitor Heitor and Daniele Dias for all the great conversations and advice that made me stronger over the years.

To all whom I have had the honor of meeting at the LMMP group during these years, for all their advice, help and friendship.

To Shell for supporting this project.

This study was financed in part by the Coordenação de Aperfeiçoamento de Pessoal de Nível Superior - Brasil (CAPES) - Finance Code 001.

Abstract

Lima, Mateus Aguiar Rodrigues de; Carvalho, Márcio da Silveira (Advisor); Benavides, Jorge Antonio Avendaño (Co-Advisor). **Controlled release of the inner content of gellan gum microcapsules using temperature as the trigger mechanism**. Rio de Janeiro, 2022. 91p. Dissertação de Mestrado – Departamento de Engenharia Mecânica, Pontifícia Universidade Católica do Rio de Janeiro.

Microcapsules are commonly used as vehicles for on-demand delivery of active contents. The capsule protects the internal content from interference of the external environment and deliver it in a controlled manner. In addition to being widely used in the pharmaceutical, food and cosmetic industries, microcapsules can be also a viable solution in medicine and in the petroleum industry to replicate themselves as cells in the body or optimize oil recovery, respectively. However, the use of a microcapsule implies the use of a shell that, due to the urge for sustainability, needs more than ever to be a biodegradable substance.. In this work, we present a method of controlled release of actives protected by a biodegradable gellan-based microcapsule using temperature as the trigger for its destruction. The study shows the effect of physical properties of the capsules in the delivery time of their internal content and how the release behaves with the increase of the heat rate involved in the process. Microcapsules were produced with flow-focusing microfluidic devices with diameters variying between 190 and 510 μm while the shell thicknesses varied between 4 and 50 μm. The study shows that, in addition to the size, the shell material influences the release behavior. In addition, another important point is how the gellan gum nature affects the thermal trigger event, since the results show that when gellan is in its deacylated form (low-acyl) it is more resistant to changes, but when its natural form (high-acyl) is added to the chain, it becomes more sensitive to the trigger mechanism until a thickness-diameter ratio threshold, where the degradation behavior changes and the delivery is delayed. The results of this work indicate that one of the possibilities for the application of gellan microcapsules is in the oil recovery process, since its shell is resistant and stable until reaching high temperatures, thus acting as a transport agent until it comes into contact with the oil at well temperature, releasing its contents.

Keywords

Microcapsules Controlled release Gellan gum Temperature

Resumo

Lima, Mateus Aguiar Rodrigues de; Carvalho, Márcio da Silveira; Benavides, Jorge Antonio Avendaño. **Liberação controlada dos ativos de microcápsulas de goma gelana utilizando temperatura como gatilho**. Rio de Janeiro, 2022. 91p. Dissertação de Mestrado – Departamento de Engenharia Mecânica, Pontifícia Universidade Católica do Rio de Janeiro.

Microcáspulas são comumente utilizadas como veículos para a entrega de ativos em locais de interesse. As cápsulas protegem seu conteúdo interno, e são capazes de liberá-los de forma controlada. Além de ser muito utilizada na indústria farmacêutica, alimentícia e cosmética, elas também são uma solução viável na medicina e na indústria de petróleo para se replicarem como células no corpo ou otimizar a recuperação de óleo, respectivamente. No entanto, a utilização de microcápsulas implica em usar uma casca que, devido a urgência pela sustentabilidade, precisa mais do que nunca ser uma substância biodegradável. Neste trabalho, apresentamos um método de liberação controlada de ativos protegidos pelo bio-polímero de goma de gelana utilizando o gatilho de temperatura como ativador da destruição da cápsula. O estudo mostra a diferença que as propriedades físicas das cápsulas causam no tempo de entrega do seu conteúdo interno e como a liberação se comporta com o aumento da taxa de calor envolvida no processo. O controle das propriedades foi realizado através da produção de microcápsulas por microfluídica ao qual os diâmetros variaram entre 190 e 510 μm enquanto as espessuras variaram entre 4 a 50 μm. O estudo mostra que, além do tamanho, o material da casca (gelana), influencia o comportamento de liberação, a partir de certo limite de relação de espessura-diâmetro. Além disso, outro ponto importante é como a natureza da gelana afeta essa liberação visto que os resultados mostram que, quando a gelana está em sua forma desacilada (low-acyl) ela é mais resistente à mudanças, porém quando sua forma natural acilada (high-acyl) é adicionada à cadeia polimérica da mistura, a composição torna-se mais sensível ao gatilho até um certo limite de razão espessura-diâmetro, alterando o comportamento da degradação e a entrega é atrasada. Os resultados indicam que uma das possibilidades de aplicação de microcápsulas de gelana é o processo de recuperação de óleo, pois sua casca é resistente e estável até altas temperaturas, dessa forma servem como agente trasportador até entrar em contato com o óleo à temperatura de poço, liberando seu conteúdo.

Palavras-chave

Microcápsulas Liberação controlada Goma gelana Temperatura

Table of contents

List of figures

List of tables

List of Abreviations

Greek Symbols

ϕ_i - Injection capillary diameter

ϕ_c - Collection capillary diameter

ρ - Density

σ - Interfacial tension

μ - Viscosity

Acronyms

HA - High-acyl

LA - Low-acyl

O/W - Oil-in-water emulsion

W/O - Water-in-oil emulsion

W/O/W - Water-in-oil-in-water emulsion

O/W/O - Oil-in-water-in-oil emulsion

D_e - External diameter

l - Distance between the injection and collection capillary

D_i - Inner diameter

r_1 - Inner radius

r_2 - External radius

O_o - Continuous oil phase

O_i - Inner oil phase

D-1 - Microfluidic device 1

D-2 - Microfluidic device 2

t - Shell thickness

t/D - Thickness-diameter ratio

Q_o - Outer flow rate

Q_i - Inner flow rate

Q_m - Middle flow rate

OT - Optimum trigger temperature

T - Temperature

1
Introduction

1.1
Motivation

A microcapsule is a micrometer-scale particle, gas bubble, or liquid drop that is surrounded by a shell [10]. They are promising candidates for protection, transportation, delivery, and controllably release of active ingredients. Through the years, microencapsulation controlled techniques have been improved to perform in different areas for encapsulation of cosmetic components, building materials, food additives, pharmaceutical products, agricultural odors [10, 11, 12, 13, 14]. Figure 1.1 shows most of the appllication fields which studies the microcapsules.

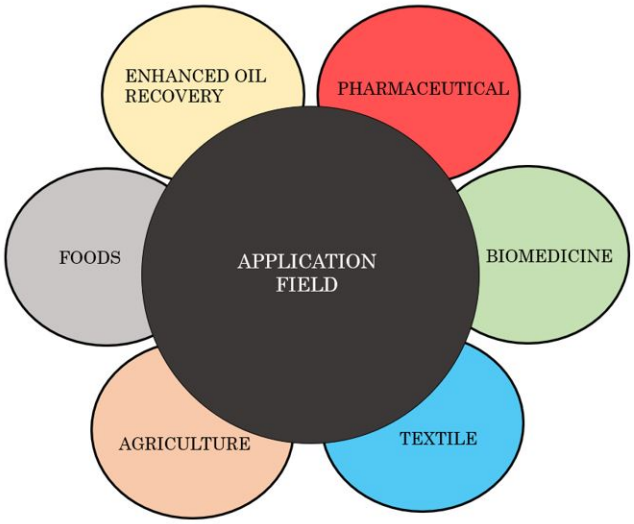

Figure 1.1: Application field of microcapsules

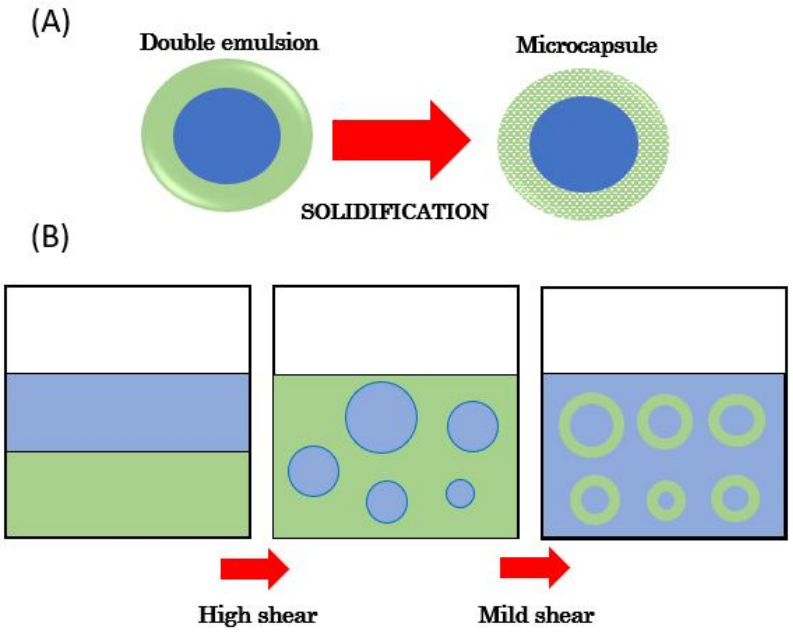

Figure 1.2: Sketch of the solidification of double-emulsions (A) and two-steps method to produce them. (B1) Two immiscible phases. (B2) Simple emulsions produced by high shear mixing. (B3) Double-emulsion template created after using shear conditions to avoid disruption of the inner phase.

There are several techniques to fabricate microcapsules, such as: spray drying, coacervation, polymerization, polymer phase separation and layer-by-layer separation [10, 11]. Most of these techniques usually requires a two-step emulsification procedure, as sketched in figure 1.2. First, a simple emulsion is formed from high shear mixing of two immiscible phases, generating water-in-oil (W/O), or oil-in-water (O/W) emulsions, always with an inner drop dispersed in the continuous phase.Then, a double emulsion is formed using milder shear conditions to avoid the disruption of the inner phase. However, these steps generate particles with varied and distributed sizes.

Therefore, in order to produce tailored microcapsules, different techniques are needed. Flow focusing devices using microfluidics enables the production of monodispersed double emulsions in just one-step method, as the internal and middle phase jets break when the three fluids involved meet in the flow, at the tip of the collection capillary, as shown in figure 1.3. The breakup is governed by the balance between the pinning, drag, and capillary forces acting in the tip of the injection capillary [2, 15]. Microfluidics techniques are ideal for manufacturing monodispersed microcapsules with controlled diameter and shell thickness [16, 17].

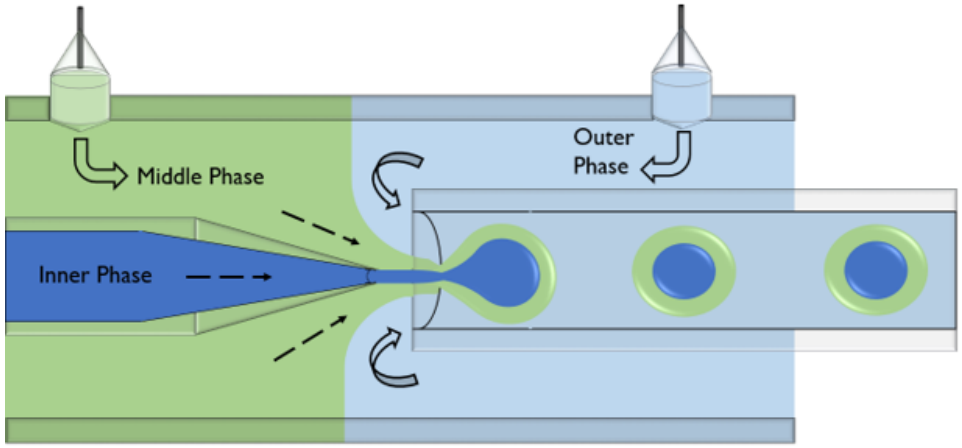

Figure 1.3: Droplets formation through microfluidics.

In most of applications mentioned before, the shell is required to be protective but depending on external conditions, the shell may be ruptured leading to the release of the inner content. The stimuli responsive microcapsules [18, 19] have drawn attention worldwide because it can be conveniently used to the controlled release of molecules at a specific site and time by using an external stimuli such as temperature [8], light [20], external stress [7, 13], pH [6], osmotic pressure [21, 22].

Environment regulations increase the demand for biodegradable components in the industry [12, 23, 24]. Nowadays, using biopolymers is a promising innovation because reaches the most diverse fields with the extra benefit of its biodegradation capacity. Thus, the development of biopolymer-based microcapsules has been the subject for many studies [25, 26].

This work adopts gellan gum as the biodegradable component of the microcapsule shell and studies its behavior under a temperature trigger event. This trigger was studied because it could fit in possible applications of enhanced oil recovery, since gellan gum is a thermosensitive substance and its gelled form can resist high temperatures, matching those at the well region. In this way, gellan-based microcapsules would apply their purpose of releasing their inner contents when encountering a body that has a temperature high enough to destroy the shell.

1.2 Dissertation goals

The main objective of this work is to develop biodegradable gellan-based microcapsules that release their inner content in a controlled way when the environment at which they are suspended reaches a certain temperature. We produced capsules with different sizes and shell thicknesses by microfluidics

to evaluate the effect of the physical parameters on the inner content release time. First, we evaluated the minimum temperature so that the capsule shell is destroyed and, from there, we evaluated how the increase in temperature accelerates this process. Furthermore, we mixed different types of gellan in the shell material to study the effect of shell formulation on the release time.

1.3 Work scope

This document is divided into six chapters. Chapter 1 introduces the main theme of this dissertation such as objectives and its structure division. Chapter 2 presents the state of the art on basic concepts such as microcapsules production, triggered release approaches and some controlled release methods. It gives an overview of how double emulsion templates are created and how microcapsules technologies are available in many applications. We also highlight the commercial value of the biopolymer gellan gum, that forms the shell composition of the suspensions.

Chapter 3 addresses how gellan capsules were produced. In this chapter, we rely on previous works to reproduce the results obtained. In addition, we adapted production by building new devices enabling production with different diameter and shell thickness. Furthermore, we showed differences in the operability window between the two types of gellan used in this work .

In Chapter 4, a detailed description of the procedure developed to disintegrate gellan gum microcapsules is presented. It includes the materials used, the set-up, and how microcapsules' diameter and shell thickness influence the release behavior of their inner content. Also, we discuss the optimum trigger temperature at which the controlled release can be manipulated with two methods: fixed temperature and variable temperature protocol. Then, a modification on the gellan composition is evaluated to analyze how an elastic form of the gellan gum alters the release behavior.

Chapter 5 presents the final remarks and suggestions for future work.

2
Literature Review

The main concepts presented in this literature review chapter are related to the structure of the microcapsule, how it can be formed, with particular attention to the double emulsion template, and how it can deliver its internal content in a controlled manner through reactions generated by an external trigger. This chapter also details the concepts of the substance chosen to be used as a capsule in this work.

2.1
Microcapsules

Microcapsules are formed by a core material involved by a membrane, also called shell or carrier [27], while the inner component is called internal phase, cargo, active or payload, as presented in figure 2.1. They are often made from double, or single, emulsion droplets that later are transformed into capsules [11]. Microencapsulation is a technique that builds a functional barrier between the core and the continuous phase to avoid chemical and physical reactions and to maintain the biological and physicochemical properties of core materials [19].

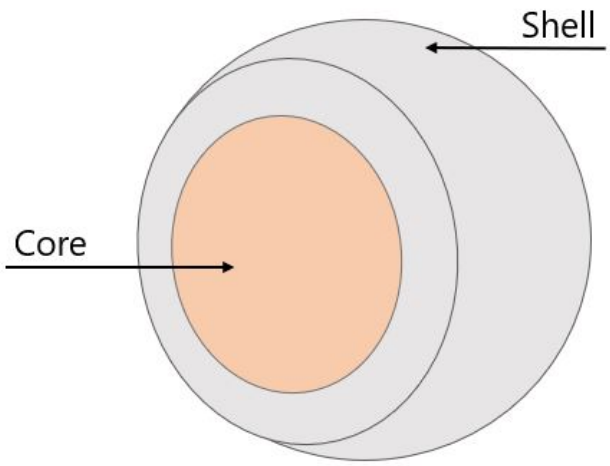

Figure 2.1: Example of a microcapsule scheme with its core and shell

Shell wall materials, used commonly for the microencapsulation of oils,

include synthetic polymers and natural biomaterials (usually carbohydrates and proteins) [19]. Their selection and the microencapsulation technique affect the properties of the microcapsules produced. According to Gharsallaoui *et al.* [28] different types of particles (fig. 2.2) can be obtained. The morphology of microcapsules can be described as mononuclear (fig. 2.2.A), poly/multinuclear (fig. 2.2.B), matrix (fig. 2.2.C), multi-wall (fig. 2.2.D), and irregular (fig. 2.2.E) [19, 14, 27, 29, 30]. Physical properties (diameter, thickness, volume) of microcapsules are usually defined by the wall material and the methods used to produce them [19, 31], they also rule the degree of protection for the core, as well as the stability of the capsule.

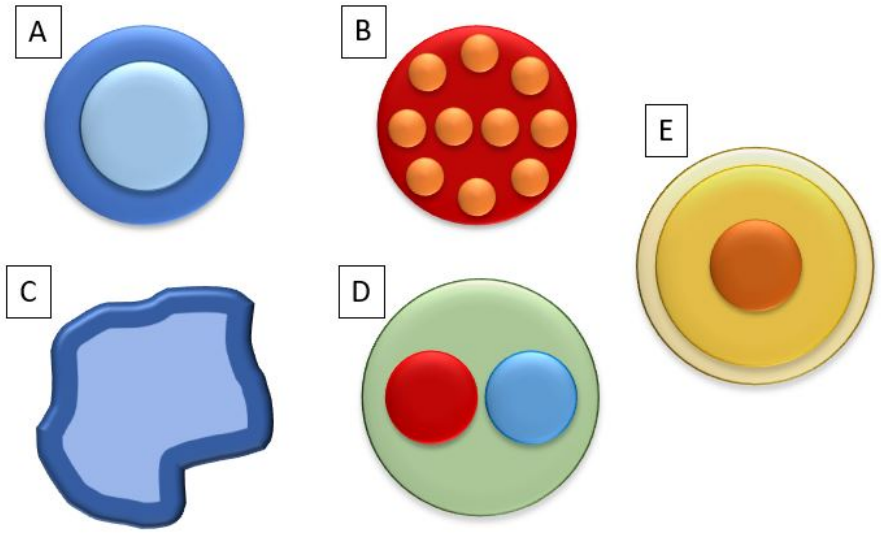

Figure 2.2: Different kinds of microcapsules.(A) single-cored, (B) matrix, (C) irregular, (D) multi-cored and (E) multi-walled microcapsule.

One of the first researches in the field of microencapsulation were conducted in the 1930s by the US company National Cash Register Co., of Dayton, OH. The researcher of NCR, Barret K. Green, developed the training system of microcapsules through the coacervation process. The first commercial application occurred in 1954, applying to carbonless copy paper, revolutionizing the business world. This paper was covered by a thin layer of microcapsules, which contained a colorless paint. This thin layer was then coated with a reagent, also colorless. When writing, i.e, when pressing the surface of the paper, the microcapsules broke, releasing the colorless paint which, upon entering contact with the reagent, it became colored, producing on the bottom sheet a copy of what was being written or drawn on the first paper. Since then, microencapsulation improve the development of new and existing products in industry such as cosmetic, textile, food, biomedical and

pharmaceutical, for example [32].

The industry of cosmetics uses microcapsules containing vitamins, skin-care agents, anti-aging products, repellents designed to transfer the active when it makes contact with human skin[33] resisting washing cycles and thus controlling the delivery of the ingredient. They also use microcapsules to conserve essential oil fragrances by avoiding heating, oxidation, and evaporation [34, 35].

In the biomedicine area microcapsules are a promising technology as they are used as artificial cells containing bioadsorbents and enzymes, by removing toxins, or drugs, from the blood of patients being much more effective when compared with standard hemodialysis[36]. There are also applications that evaluated a challenging microencapsulation of mammalian cells [37, 38, 39] for use in musculoskeletal, neural, and cardiovascular tissue engineering and tumor therapy.

The food industry has developed interest in microencapsulation technology to solve problems associated with ingredient that are environmentally unstable, allowing sweeteners, colorants, vitamins, probiotics to be incorporated into different beverages and foods in general. Thus, this technique can protect active compounds from processing the food to gastrointestinal environment in the human body [14, 31, 40, 41].

Another application of microcapsules is found in the pharmaceutical industry, where a priori it is easier to identify this system, as society consumes capsules as medicine, from being able to cure side effects to regulate the hormonal system in the body [31, 42, 43, 44].

Other technological applications of this technique are found in the agricultural sector, which can work as an alternative to dangerous pesticides as they release pheromones that will disrupt insects mating process. They can also be used as a selfhealing method for asphalt paviments[14, 12, 45]. In addition, recent studies have shown advances in the application of microcapsules in the process of enhanced oil recovery as fluid mobility agents that can lead the redistribution of the flow within the porous media. Also, they can carry surfactants that could react and clear the flow path resulting in increased volumes of recovered oil [13, 45, 46].

Thus, capsules are very relevant in several areas of industry and are also present in people's daily lives. In certain applications, the objective is not always to release the inner content, but to protect it for long periods. On the other hand, in most cases, there is a need to destroy them in a controlled manner. Therefore, it is extremely important to know the chemical and physical characteristics of the capsule, and its release kinetics that can guarantee delivery and be able to apply it correctly.

Commonly used methods of microencapsulation are shown in fig. 2.3. The coacervation process (fig. 2.3.A) utilize the electrostatic association of two oppositely charged reagents at liquid/liquid interfaces producing a thin shell. The emulsification polymerization process (fig. 2.3.B) yields a polymer shell wall around a stabilized droplet by the same polymer deposited at an aqueous interface. The layer-by-layer (LBL) assembly method (fig. 2.3.C) uses metal oxide particles suspended in an aqueous solution, then oppositely charged polyelectrolytes are deposited onto the particles, forming multi-layers of polymers held together by electrostatic interaction. Another method of preparing microcapsules is the internal phase separation (fig. 2.3.D) in which a polymer is dissolved in a core material with a volatile solvent and precipitates, migrating to the aqueous/organic interface, thus creating the polymer shell wall. Another way to produce micropasules is through the double emulsion templates that can be converted into capsules through solidification methods achieved through polymerization of monomers, cross-linking of polymers, or through solvent extraction [1, 11]. The production of microcapsules by double emulsion templates, through microfluidics, is very relevant because it enables the production of monodispersed capsules, increasing the repetition results and their degree of reliability.

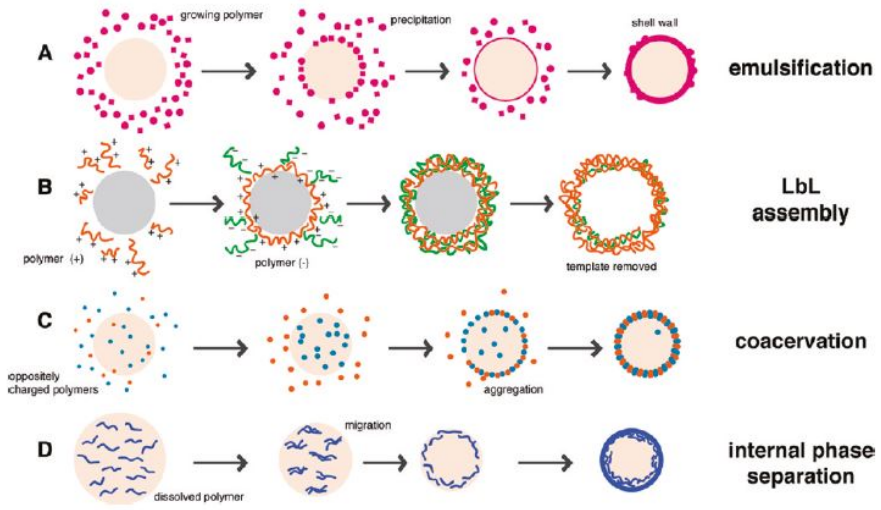

Figure 2.3: Dynamic self-assembly methods of microcapsules containing "on-demand" cargo: (a) an emulsification polymerization; (b) layer by layer assembly of polyelectrolytes (c) coacervation of two oppositely charged polymers (d) interphase separation. Adapted from [1].

Hence, as a way to control these physical characteristics of microcapsules, one of the best ways to achieve it is through flow focusing devices. Through microfluidic devices, the microencapsulation is done by double emulsions

templates, to which the fluids flow separated from each other and then meet at a specific location in order to produce this double emulsion. From that point, the gelation/solidification processes of the intermediate phase begins and then the microcapsule is formed.

2.2 Emulsions

An emulsion is a mixture of two immiscible liquids in which one of the phases is dispersed as droplets within the other, known as continuous phase, as shown in fig. 2.4. The criteria to create an emulsion is the presence of two immiscible liquids, at least a surface-active component as the emulsifying agent, and an external energy, to disperse one liquid into another as droplets.

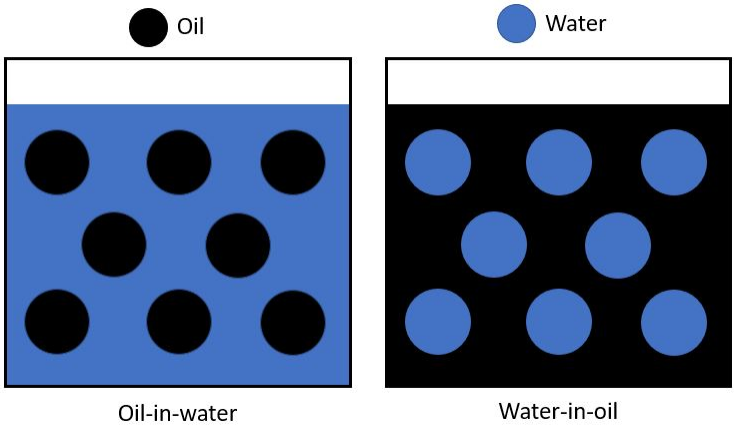

Figure 2.4: Example of simple emulsions template: oil-in-water (O/W) and water-in-oil (W/O).

A system that contains three immiscible phases instead of two is called a double, or complex, emulsion, which is very common in the production of microcapsules. Complex emulsions, shown in fig. 2.5, can be divide in two types: oil-in-water-in-oil (O/W/O) and water-in-oil-in-water (W/O/W). In the first one, inner and outer phases are oil-based emulsion while for the second one the inner and outer phases are water-based emulsion [47, 48].

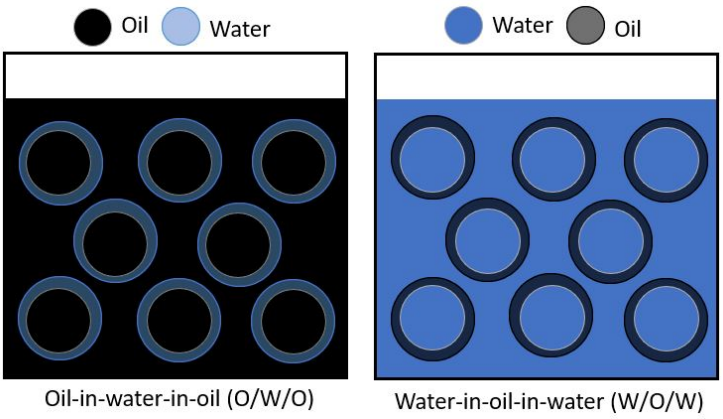

Figure 2.5: Example of double emulsions templates: oil-in-water-in-oil (O/W/O) and water-in-oil-in-water (W/O/W).

Emulsions are thermodynamically unstable, kinetically stable [49, 50, 51, 52, 53]. To be considered stable, an emulsion has to resist physical changes over a length of time [54]. Generally, emulsions are stabilized by an emulsifier, which is usually a surfactant that promotes stabilization. Stabilizers act adsorbing to the water-oil interface promoting stability by reducing the interfacial tension during emulsion formation [54, 55, 56, 57].

The nature of the emulsifier added to the mixture dictates the type of emulsion formed. Bancroft rule states that the phase in which an emulsifier is more soluble constitutes the continuous phase of the emulsion [58, 59, 27, 29]. In general, if a hydrophobic surfactant is used, it tends to form a water-in-oil emulsion. On the other hand, if a hydrophilic surfactant is used, it tends to form an oil-in-water emulsion.

2.3 Microfluidics

The capsule behavior depends on the mechanical and chemical properties, the permeability of the shell, which in turn are tunable by the capsule size, shell thickness, and composition. For controlled and target release, encapsulation systems that provide fine control over these parameters are often desired. Interfacial polymerization, self-assembly, or coacervation processes usually leads to very polydispersed microcapsules and consequently to uncontrolled release characteristics [60, 61, 62, 63, 64].

One route to overcome these difficulties is the use of microfluidics to produce monodispersed double emulsions templates. Subsequently solidifying the middle phase yields solid-shelled microcapsules. The interfacial tensions between the different fluids force the drops to be spherical; moreover, the drop

sizes are determined by the shear forces exerted on the flowing fluids, which can be carefully tuned in a microfluidic device [10].

Microfluidics has often been considered as an important development in sciences research and industry [65, 66]. It is a field that has seen a great deal of research in recent times with the development of new devices, with a geometric scale between 100 nm and 100 μm [65, 67] that are capable of outperforming macroscopic processes. However, despite the great deal of works it is commonly refereed as an "on going" discipline that it is not matured yet [65, 68].

Some relevant studies show that through microfluidics one can produce emulsions/microcapsules with tunable mechanical properties. Amstad [11] showed the degree of control over the drop size is low if the drops are formed through mechanical agitation using rotor-stator systems or high-pressure homogenization but it is higher if drops are formed using membranes and even higher if they are formed with microfluidics. Basically, the degree of control depends on the technique used to fabricate drops.

Utada et al. [2] developed a microcapillary device for generating double emulsions in a single step (fig. 2.5) allowing control of the outer and inner drop sizes. It consisted of two cylindrical glass capillaries, one for injection and the other for collection, placed into the opposite ends of a square glass capillary. Within this device, an inner fluid flows through the injection capillary and is embraced by a second immiscible fluid (middle phase) that flows through the interstices between this cylindrical capillary and the square one. The middle phase is engulfed by a third fluid (outer phase) flowing in the opposite direction through the interstices between the collection tube and the square one. Thus, the collection capillary will be the place that the W/O/W or O/W/O templates will be formed.

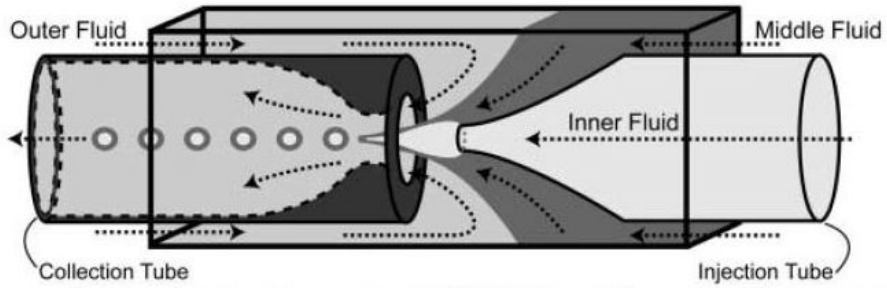

Figure 2.6: Microcapillary geometry for generating double emulsions from coaxial jets. Adapted from [2].

There are two kinds of flow regimes: dripping and jetting, both capable of forming double emulsion templates. The first one produces droplets near the capillary collection entrance while the second form drops downstream. The

dripping regime, shown in fig 2.7, tends to produce monodispersed emulsions while the jetting regime is quite irregular leading to a more polydispersed production.

Michelon et al. [3] studied the production of gellan capsules through several microfluidic devices with different geometries, and was able to manipulate the shell thickness and size of the particles by altering the flow rates of the inner, middle and continuous phase. If the flow rate of the phases is outside the operability limits of the process, monodispersed capsules with a single core are not produced.

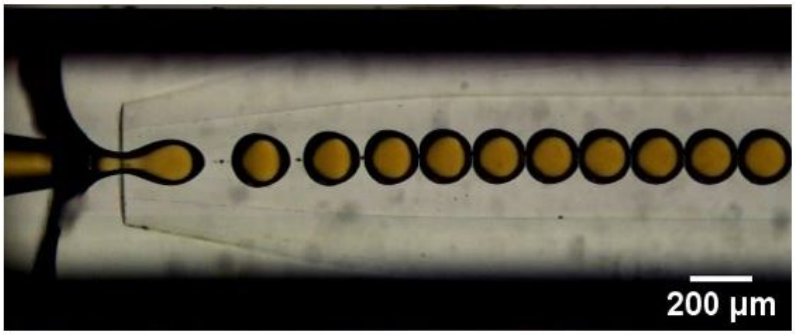

Figure 2.7: O/W/O template formation in the ideal intermittent dripping regime [3].

As negative points, microfluidics is not appropriate to form very small capsules (below 50 μm) and have a low throughput. In order to produce very small capsules, the diameters of the capillary tubes would need to be very small and the working pressures would be very high, thus resulting in the internal destruction of the device and destabilization of production[10]. Attempts to accelerate production are being studied. Alternative fabrication technologies, such as 3D printing, rapidly advance and open up new possibilities to the fabrication of more advanced devices [11].

2.4 Gellan Gum

The application of microcapsules is strongly related to the materials used to build their shell. Different triggers can only be applied if the ideal type of material for that specific application is present [11]. Thus, before starting the application, it is necessary to understand the material that will make up the shell. One commonly used material as shell production is gel [5].

Gels are soft semi-solid materials that consist of components that act as the solvent and gelator, i.e, the gelling agent [69]. The gelling phenomenon happens when the solvent molecules penetrate a hydrocolloidal network formed

by the gelator, which itself can be of several types, some imparting elasticity while others, including inorganic particulate gels, easily permit disruption. Some gels, as in hydrogels, can crosslink physically or be covalently cross-linked in which case the crosslinking agent can be seen as a gelling agent [70, 71, 72, 73].

A biocompatible polymer capable of forming stronger and less permeable hydrogels is used in this work: gellan gum [74]. It is a linear, anionic, negatively charged exopolysaccharide, biodegradable and non-toxic in nature. It produces hard and translucent gel, and stable at low pH [75]. Gellan gum is commercially prepared by microbial fermentation from bacterium Sphingomonas elodea and was approved for food use by the FDA in 1992 [4]. Kelco [76] identified its commercial potential.

Gellan gum is available in two forms [4]: the deacetylated form, known as low acyl (LA) gellan gum, and the acetylated native form, known as high acyl (HA) gellan gum. Figure 2.8 shows the chemical structure for both forms. The low acyl form is the most common and most commercially available [77]. This form produces stronger and brittler gels while the high acyl form generates more elastic and weaker gels [25]. High acyl gellan gels are weaker due to their acetyl and glyceryl groups, as shown in fig. 2.8, presence in its composition [4]

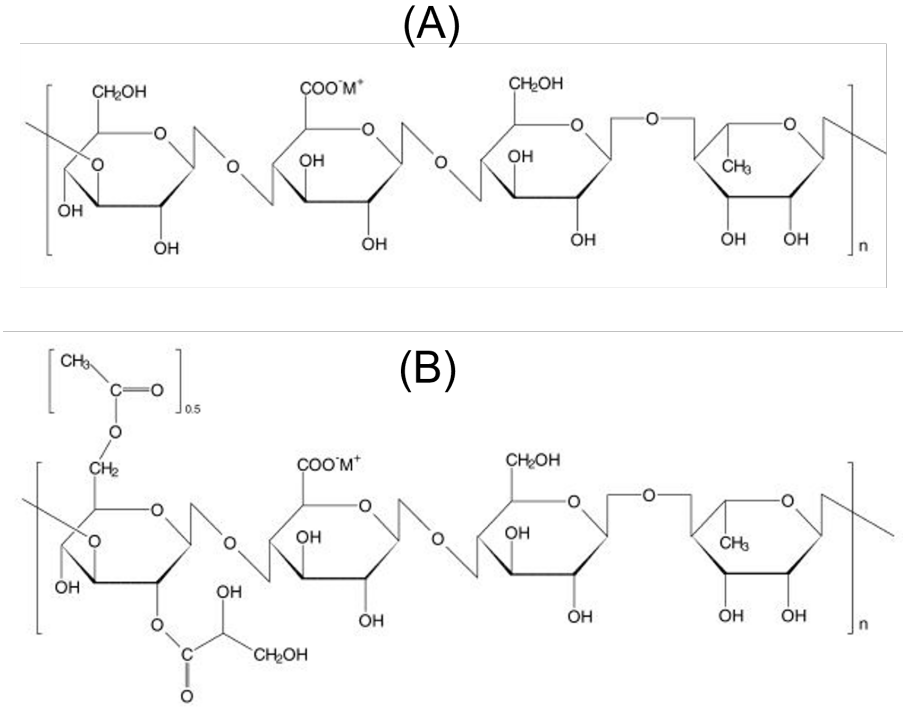

Figure 2.8: The chemical structure of gellan gum: (A) native form (high acyl); (B) deacylated form (low acyl) [4].

Gellan gum is a thermoresponsive polymer, exhibiting upper critical

solution temperatures [78]. Low acyl gellan dissolves in water at temperatures above 80°C while high acyl gellan solutions gel at much higher temperatures [4]. Figure 2.9 shows the transformation of the gellan gum from aqueous solution, transitioning from a disordered solution state to a gel state upon cooling as the coil to double-helix transition occurs [79, 80]. Then aggregation of helical sequences is necessary to form a true gel. Gelation occurs by aggregation of double helices. Aggregation stabilises the helices to temperatures higher than those at which they form on cooling, giving thermal hysteresis between gelation and melting. Melting of aggregated and non-aggregated helices can be seen as separate thermal and rheological processes [76]. Cations stabilize gel structures by an ionotropic process, connecting the double helix chains [78], and are responsible for the gelation temperature as molecular weight and processing conditions as well [81].

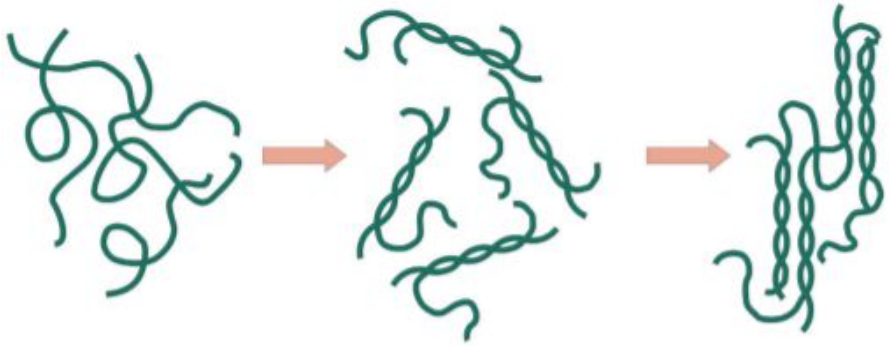

Figure 2.9: Gradual transformation of gellan gum from aqueous solutions. [5]

The gelling process is different depending on whether the type of cation is mono or divalent[75, 76, 82, 83]. For divalent, the gelling efficiency is increased in relation to monovalent cations because they can promote additional bonds with the carboxylated groups of the gellan gum chains and are induced to be more thermally stable.

Very high salt concentration or very acidic environments, or both, cause excessive aggregation and weaken the gel [76].

One of the applications that gellan gum has is the potential in biomedicine area where studies for tissue engineering have been made through the years [82, 84]. Gellan gum can be mixed with other polymers and reinforced with cations. It can promote the treatment of cartilage regeneration, be used to protect cells from mechanical forces experienced in vivo, and artificially implant a bone-like layer to replace cartilage with no immune responses from the immunological system [85].

As already mentioned in this section, gellan gels can resist acidic environments and, due to their transparency, they do not affect the appearance of

foods [86]. It can be resistant to high temperatures, suitable for activities, like baking a cake. Gellan gum is used as a transportation [76] of flavors as well and retains tastes of seasonal foods and it is also used to stabilize ice creams.

The first record of promoting gellan gum as capsules was in 1996, where Alhaique *et al.* [86] studied the preparation of gel capsules and its controlled release. The microcapsules were able to be produced by gelation of gellan gum around drops, calcium chloride, and a model drug. The delivery study showed that the rate of delivery in water is mostly affected by solvent uptake due to the weight rise of the microcapsules.

Michelon *et al.*[3] have successfully controlled the production of gellan-based microcapsules. They discuss the production of microcapsules with hydrogel-based shells by ionotropic gelation of gellan gum from monodispersed oil-in-water-in-oil (O/W/O) double emulsion templates obtained using glass capillary microfluidic devices. This study reports the operability window for the production of monodispersed microcapsules as a function of the flow rate of each fluid phase and the dimensions of the device. Microcapsules were produced with mean diameters ranging from 95 to 260 μm. The main results showed that one can independently control the capsule diameter and shell thickness by varying the outer and middle phase flow rates. They also report an oil extraction step for the shell gelation in order to disperse microcapsules in an aqueous medium

2.5 Controlled release

As mentioned before, capsules are means of transport for active storage and can deliver substances at a specific time and condition to affect the outcome of larger systems. Triggering is a phenomenon that depends on the stimuli, thus the development of appropriate initiators plays a key role in the release of capsule contents to provide the desired response. The release of capsule cargos has been developed with chemical and physical methods. Capsule systems are particularly appealing for the delivery of small molecules and particles.

2.5.1 Shell wall release mechanism

The approaches for shell wall desintegration can be separated into physical changes, in which phase transitions and/or mechanical disintegration mechanisms dominate, and chemical changes, in which chemical reactions destroys the shell. Physical rupture of capsules embedded in solid materials

induced by cracking of the material is used in odorants, self-healing materials [33, 34, 45], and carbonless copy paper [87].

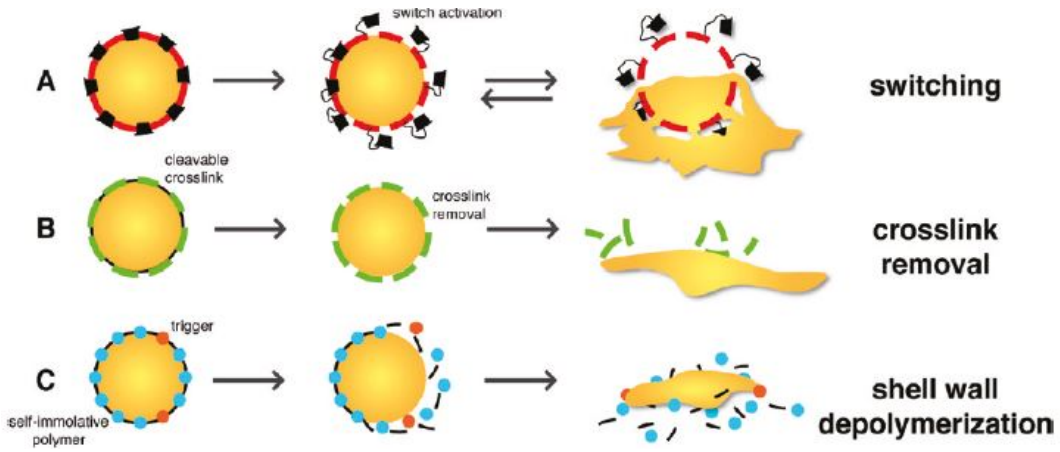

Figure 2.10: Methods for the chemical disassembly of microcapsule shell walls: (A) switching mechanism, (B) cross-link removal, and (C) shell wall depolymerization [1].

The chemical control approach, as shown in fig. 2.10, over shell wall desintegration offers many advantages for designing drug-delivery and self-healing systems. Chemical mechanisms can be divided into three major categories: shell wall switching reactions; disintegration of the shell wall via chemical cleavage of cross-links; triggered depolymerization of the shell wall. The switching reaction, Fig. 2.10 (A), can be defined as instances in which the porosity of a microcapsule shell wall is controlled by structural changes rather than chemical reactions involving covalent bond formation and disruption. Stimulants such as electricity [46] and light [88] can be used to modify the porosity of a shell. The main advantage of this technique is the capsule's ability to undergo several release cycles, acting as some kind of gate, opening and closing upon command. Cross-link removal reactions, Fig. 2.10 (B), disintegrate the capsule by chemically disrupting shell wall cross-links. One of the main applied event triggers is the disassembly by hydrolysis of carbonate esters [31]. Advantages of this technique include the ability to control trigger loading and release times. The more broken crosslinking is, the faster is the release, resulting in the capacity for near-instantaneous content delivery [89]. The shell wall depolymerization, Fig. 2.10 (C), technique utilizes the triggered depolymerization of a shell wall polymer upon removal of a protecting headgroup, such as carbonate esters or carbamates [90, 91]. The advantages of this technique include a diverse set of triggers , and lower amounts of stimulants to disruption activation due to the mechanism of self-immolative polymers signal amplification [92].

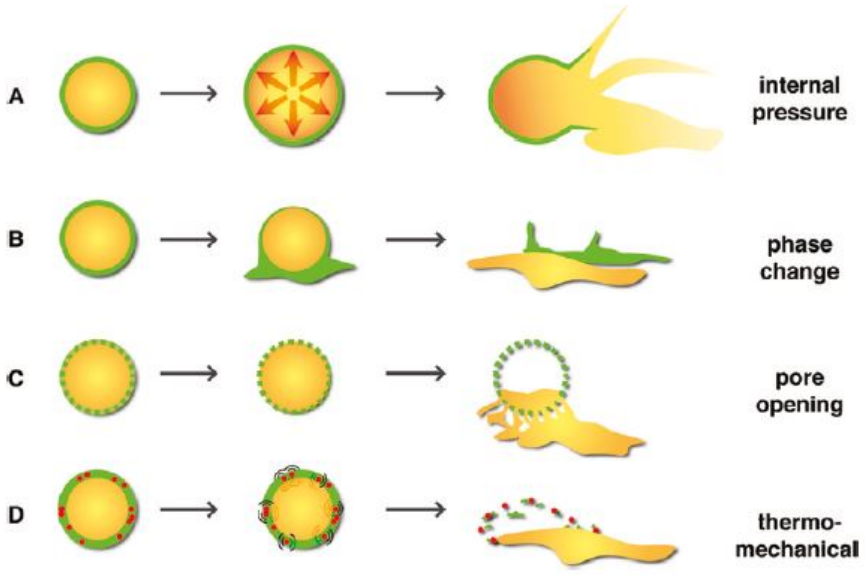

Figure 2.11: Physical methods of capsule release: (A) shell wall rupture by an increase in internal pressure, (B) melting of the polymer shell wall, (C) change in porosity of the shell wall resulting from a phase transition of a shell wall polymer, and (D) disintegration of the shell wall utilizing nanoparticles that oscillate in response to an external trigger [1].

Physical methods for inner content release are summarized in fig. 2.11. An increase in internal pressure can cause shell wall rupture, as shown in fig.2.11 (A). The goal of this method is to increase pressure from within a microcapsule shell causing its burst and is generally initiated by thermal conditions at which the inner liquid phase vaporizes, or can be initiated by the mechanical contraction of the shell wall. The shell wall melting, fig.2.11 (B), is another release control approach that occurs upon temperature increase. Thus, the shell material melts when the melting point of a polymer is low enough that melting occurs before core liquid vaporization [93]. Another interesting method is the change in porosity of the shell wall, fig.2.11 (C). Basically, the membrane wall is composed of two kinds of polymers and, upon heating, one of them shrinks while the other remains intact, allowing the creation of pores in the shell, thus releasing its contents [94, 95]. Finally, thermomechanical degradation of the shell wall, shown in fig.2.11 (D), can be caused by exposure to electric [96] or magnetic fields [13]. The disintegration can occur when the shell wall is composed of nanoparticles and oscillates in response to an external trigger, causing heating and tearing of the capsule, leading to a core release.

In this work, the trigger to activate the capsule disassociation will be the temperature. It is important to note that all the release conditions above can be consequences of the increase in temperature in the system, although some

of them could be activated by other triggers as well.

2.5.2 Trigger mechanism in shell wall release

Chemical and physical triggers have been widely studied during the past few years. Currently, chemical reactions have the largest number of citations and the approaches for shell wall disassemble with this trigger are guided by changes in pH, for example.

2.5.2.1 pH

Many chemical reactions are triggered by changing the pH of a buffer solution [89]. Abbaspourrad *et al.* [6] studied solid shells composed of pH-responsive biocompatible polymers exposed to a pH trigger. After shell-bulk contact, the polymer chains of the shell become highly charged, thus leading to a complete dissolution of the inner phase with the bulk fluid [97, 98]. The exact pH that triggers the release was set by the choice of the polymer: a base-sensitive polymer dissolves at pH > 7 while an acid-sensitive polymer, dissolves at pH < 6. Figure 2.12 represents two mixed different populations when the microcapsules are first exposed to an acidic environment, the acid-responsive microcapsules degrade and quickly release their contents. On the other hand, basic-responsive microcapsules remained stable and only reacts after turning the environment basic. Thus, by fabricating different microcapsules using different pH-responsive polymers, we can program the sequential release of different actives [95].

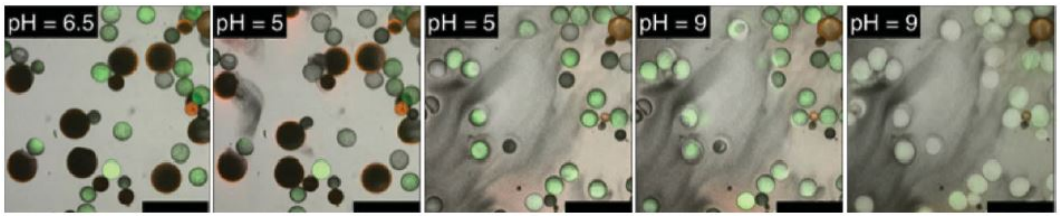

Figure 2.12: Optical micrographs, showing the release of a yellow encapsulated dye only from acid-responsive double emulsion-templated microcapsules when the pH is reduced to 5 (second and third frames). An encapsulated green dye, along with polystyrene tracer particles (grey), is then released from base-responsive microcapsules when the pH is increased to 9 (fourth and fifth frames) [6].

2.5.2.2 External stress

Externally imposed stress is an important class of stimuli for microcapsule release. Flow of suspended microcapsules through confined channels poses a challenging problem due to its complex fluid-solid interaction. Leopercio [7] showed that deformation of dynamics of soft gellan gum microcapsules as they flow through a constricted capillary, as shown in fig. 2.13 strongly depends on the capillary geometry, capsule dimensions, and propertied and flow rate. If the stress imposed by the flow is higher than what the capsule shell can sustain, it will rupture and release its internal content.

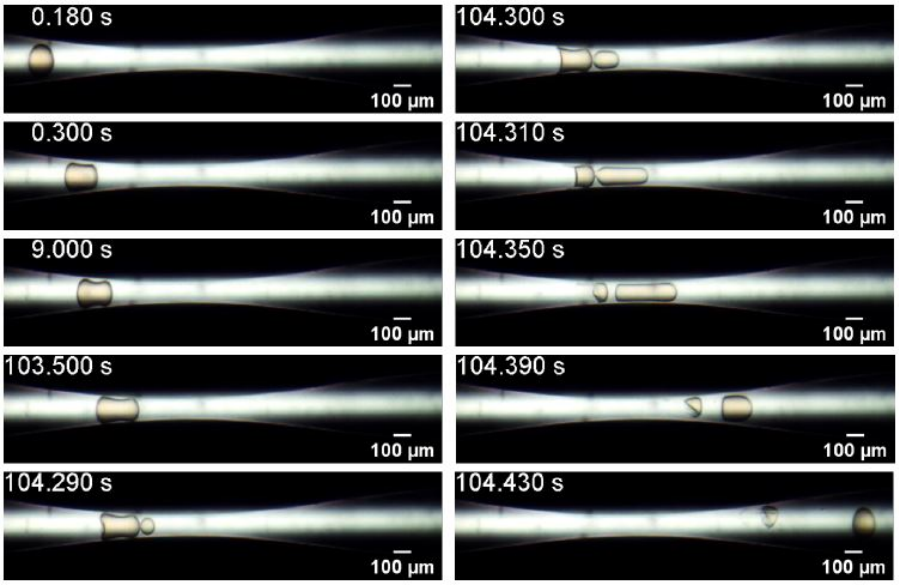

Figure 2.13: Evolution of the microcapsule position and configuration as it flows through the constriction [7].

2.5.2.3 Temperature

Another important class of trigger and the main theme of this dissertation is the release through temperature stimulus. This finds applications in transporting and releasing food additives, cosmetics, or drugs, which often require the release to be triggered at body temperature (37 °C). Lipids or hydrocarbons are a natural choice of shell material in this case. Many of them are solid at room temperature, enabling robust encapsulation under ambient conditions, but melt at temperatures in the range 30–43 °C, releasing the encapsulated active when heated [8, 10]. Jie Sun *et al.* [8] performed a microfluidic melt emulsification method for encapsulation and release of actives.

Figure 2.14: Release of toluidine blue from solid capsules of paraffin. (Frame 1) Solid capsules of paraffin encapsulating toluidine blue at room temperature. (Frame 2) When heated to 45 °C, solid paraffin shell turns into a liquid shell. (Frame 3)The inner droplet starts to coalesce with the continuous phase, releasing the toludine blue dye. (Frame 4) Toluidine blue dyes are almost entirely released after 5 mins of heating [8].

They first formed W/O/W double emulsion template and demonstrated how the actives encapsulated inside the solid shell can be controllably and rapidly released by applying a temperature trigger to melt the shell. Figure 2.14 shows how the melting process evolved. Solid paraffin-based microcapsules encapsulating toluene blue when heated above 45 °C, for 5 minutes, the shell melts. Thus, the inner droplet starts to coalesce with the continuous phase, releasing the toludine blue dye.

Amstad *et al.* [9] formed double emulsion templates with polymerosomes and the results showed that they were thermosensitive. The shell was formed from a middle oil phase composed by mixture of PEG-b-poly[lactic acid] (PEG-b-PLA) and a thermosensitive pNIPAm-b-poly[lactic-co-glycolic acid] (pNIPAm-b-PLGA) diblock copolymers. Figure 2.15.A shows the fraction of intact polymerosomes decreases with incubation time at 40 °C and how the concentration of PNIPAM-b-PGLA affects the response while at this temperature. Figure 2.15.B shows confocal micrographs for these polymersomes after 20 minutes of incubation time.

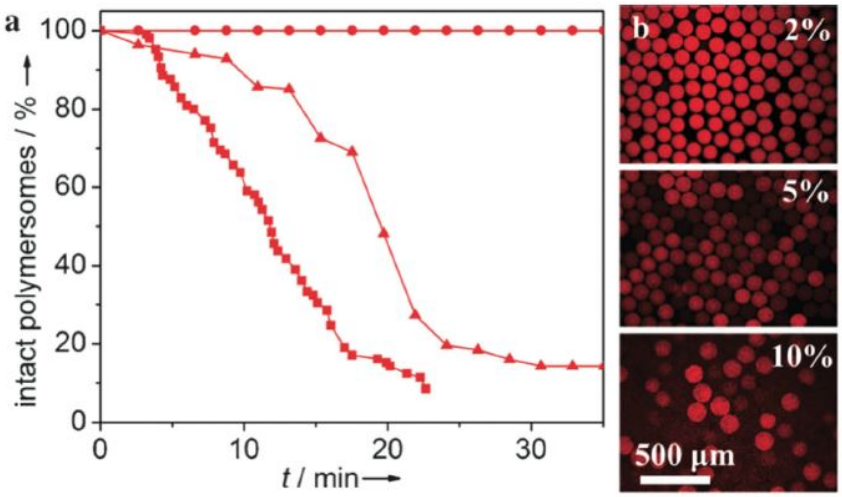

Figure 2.15: (a) Fraction of intact polymerosomes decreases with incubation time at 40 °C; circles, triangles, and squares are for PEG-b-PLA polymerosome shells including 2 wt%, 5 wt%, and 10 wt% PNIPAM-b-PLGA, respectively. Confocal micrographs for these polymerosomes after 20 minutes of incubation are shown in (b) [9].

In the present work, we study the controlled release of the inner content of gellan-based microcapsules, using temperature as the trigger mechanism. We analyze how the temperature and capsule properties (shell material, diameter and shell thickness) affect the release time. The release of the inner content is determined by adding a dye in the inner phase of the capsules and observing a suspension of microcapsules inside a controlled temperature bath in an inverted microscope. The results show how different capsules can be designed to deliver their inner content at different levels of temperature and residence time, we report two different approaches on raising the temperature of our particles and a promising trigger condition to disintegrate its shell.

3
Experimental production

3.1
Gellan microcapsules

The capsules were produced through microfluidic devices and therefore double-emulsion templates are used in this work. The templates are composed by sunflower oil in the inner and continuos phase at which they are suspended. Gellan gum aqueous solution is used as the middle phase to form a bio-polymeric and elastic shell.

The inner phase is a refined commercial sunflower oil (Liza, Cargill S.A, Brasil) with the addition of a purple or a yellow food-grade dye only for visualization purposes. It is important to mention that our focus is in the shell of the microcapsule, so this oily phase will only serve to compose our capsules as the active to be delivered.

The middle phase (figure 3.1) is prepared shortly before starting the microcapsules production and consist of a mixture of 0.5 wt% of low-acyl gellan gum Kelcogel CG-LA (CP Kelco Brasil S/A, Brazil) and 2 wt% of polyoxyethylene sorbitan monolaurete, Tween20 surfactant (Sigma-Aldrich, USA), in ultrapure water (Direct-Q3 UV System, Millipore Co., USA) with resistivity 18.2 MΩ/cm. This mixture stays under magnetiic stirring at 80 °C for 10 minutes. In addition to this intermediate phase composition, we also produced gellan modified shells with 0.5 wt%, where 95% was composed of the same low-acyl (LA) gellan gum KelcogelCG-LA while the remaining 5% was composed of high-acyl (HA) gellan gum KelcogelCG- HA (CP Kelco Brasil S/A, Brazil). The procedure was the same but the mixture temperature required is 90 °C.

The contiuous phase is a sunflower oil containing 1 wt% of calcium acetate (sigma-Aldrich, USA) and 5 wt% of polyglycerol-polyricinoleate emulsifier commercially named as Grinstead PGPR (Danisco, Brazil). Its filtering process is shown in figure 3.2.

Figure 3.1: Post-mixed liquid gellan 0.5 wt%. The modified gellan that contains both low and high-acyl forms is turbid (left), while pure gellan with only its low-acyl form is translucent (right).

Figure 3.2: Filtering process of the external phase of sunflower oil with calcium acetate

The production of microcapsules was made with hydrogel-based shells by ionotropic gelation of gellan-gum from monodispersed oil-in-water-in-oil double emulsion templates (O/W/O) using glass-capillary microfluidic devices.

As already mentioned in Chapter 2, the gelation occurs through crosslinking. These bonds are induced by cations dispersed in the external phase of production, as shown in figure 3.3. In our case, the presence of calcium acetate (Ca^{+2}) in the external sunflower oil stimulates the ionotropic process between the divalent cation and the gellan gum of the middle phase. The result of this crosslink is strong and impermeable bonds that the formed gel has.

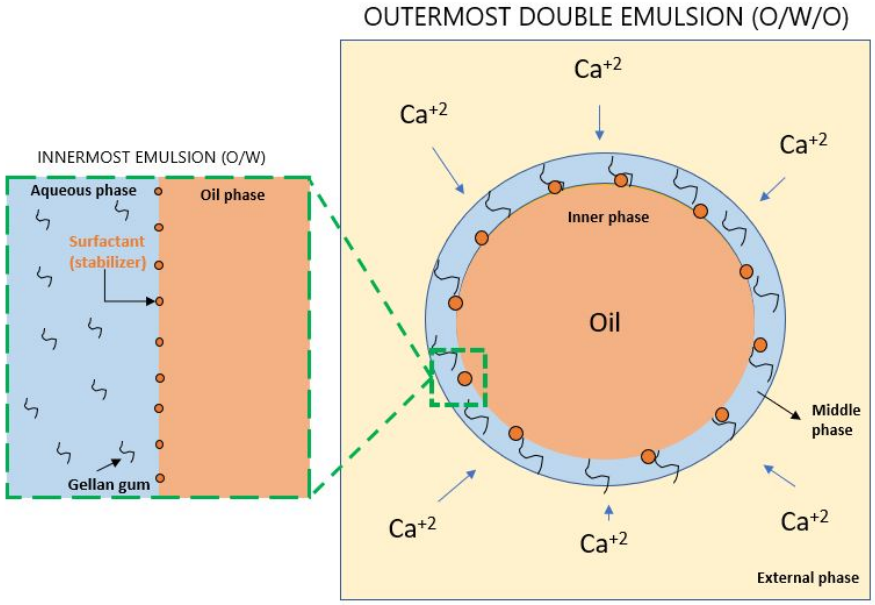

Figure 3.3: Illustration of gellan gelation by the presence of cations dispersed in the external phase

The density of each phase was measured in a digital densimeter (model DMA 4200M, Anton Paar, Austria) at 25 °C.

Using a stainless steel Couette geometry, we measured viscosity curve (μ) for the two gellan solutions used in this work with a rheometer (model DHR-3, TA Instruments, USA).

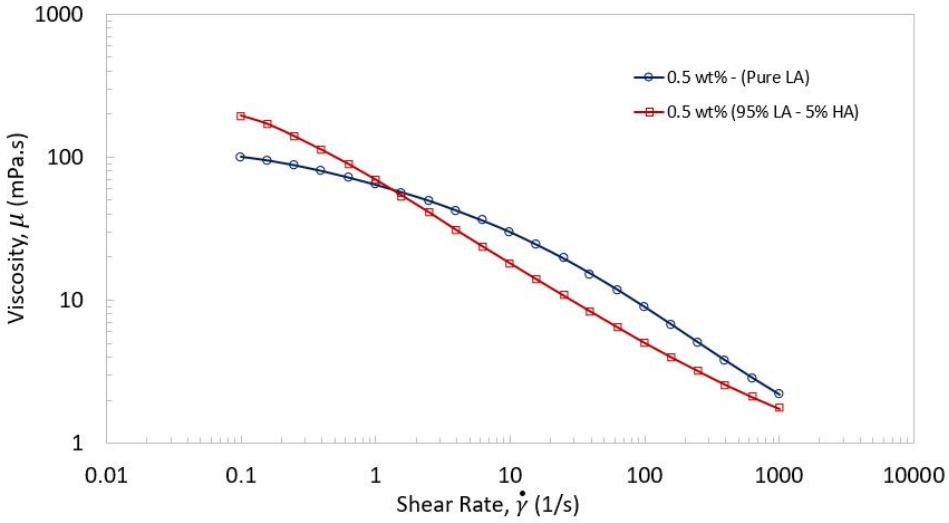

Figure 3.4: At room temperature (25 °C) the viscosity behavior with the shear rate implemented for both gellan-based mixtures of 0.5wt%.

As shown in figure 3.4 , the viscosity values of the gellan-based mixtures varies with shear rate ranging from 10^{-1} to 10^{3} s^{-1}. The non-newtonian response demonstrates a shear thinning behavior for the gellan-based mixtures acting as a pseudo plastic material, often observed in polymers solution. Despite the high-acyl (HA) addition into the gellan composition, the viscosity behavior did not have a great modification in response to the shear rate applied.

A digital tensiometer (model DCAT 25, DataPhysics, Germany) was used to measure the interfacial tensions (σ) by the Wilhelmy plate method.

The difference in the interfacial tension values (table 3.1) between the internal-intermediate and intermediate-continuous phases is explained by the presence of tween20 and PGPR surfactants.

Phase	ρ [kg/m^3]	μ [mPa.s]	σ [mN/m]
Continuous (O_O)	755.2 ± 0.1	55.3	5.4 ± 0.3
Middle (W)	1020.1 ± 0.9	2.2-100.7	
Inner (O_i)	752.8 ± 0.1	73.9	2.6 ± 0.2

Table 3.1: Interfacial tension (σ), density (ρ) and viscosity (μ) of the respective phases of the low-acyl (LA) gellan microcapsules.

Table 3.1 above summarizes the values of the properties of all the three phases, considereing the low-acyl gellan gum solution.

3.2 Methodology and experimental setup

3.2.1 Microfluidic device

Figure 3.5 shows a sketch of the three-dimensional coaxial microfluidic device [3] used to produce the double emulsion templates. This device makes possible generate O/W/O double emulsions templates precisely controlling the inner and outer drop sizes as discussed previously. The injection capillary (left, figure 3.5) has a smaller inner tip diameter (ϕ_i), on the order of 10^1 micrometers, while the so called collection capillary (right, fig.3.5) has an inner tip diameter (ϕ_c) of the order of 10^2 micrometers.

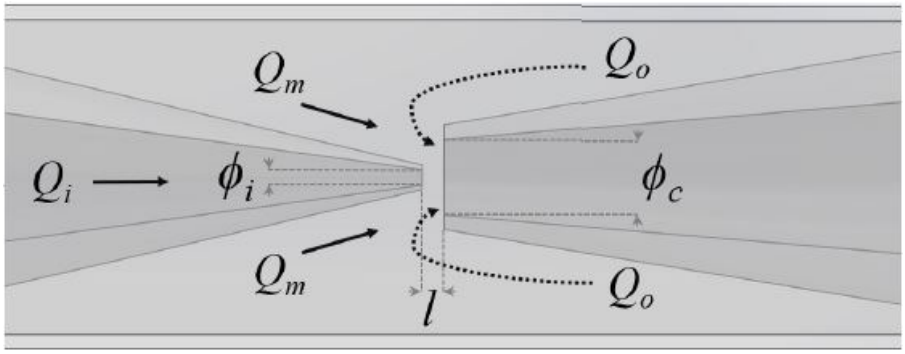

Figure 3.5: Detailed schematic of the collection and injection capillaries within the square capillary of the device [3]. $\phi_{i,c}$ are the injection and collection capillary diameters; $Q_{i,m,o}$ are the inner, middle and outer flow rates; l is the distance betweenn the capillary tips.

A detailed description of the device structure is presented by Michelon *et al.* [3] and Leopercio [7]. In summary, a squared capillary is fixed to glass slide with an epoxy resin. The cylindrical glass-capillaries are inserted, and fixed, into the opposite ends of the square capillary. Then, the cylindrical capillaries are precisely align in order to make a coaxial geometry. Nabavi *et al.* [15] predicted the different controlled drop formation modes (dripping/jetting regime). These modes are related to the distance (l) between injection and collection capillaries, as shown in figure 3.5. Finally, three stainless steel needles are used to dispense and connect the fluids into the system.Figure 3.6 presents a photograph of one of the devices used, indicating the inlet needle for all the three phases.

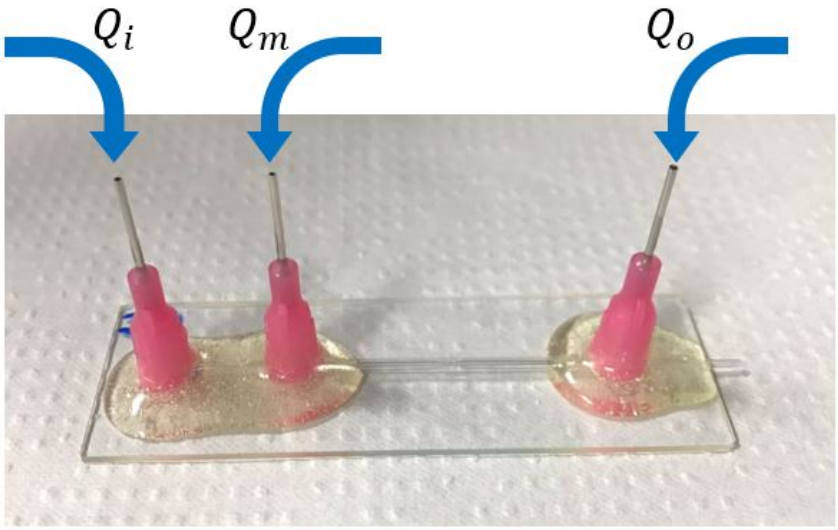

Figure 3.6: Microfluidic device.

To produce the desired microcapsules, the inner phase flows (Q_i) through the injection capillary, while the middle (Q_m) and continuous phases flow (Q_o) through the interstices between the cylindrical and square capillaries, as sketched in figure 3.6.

In addition to producing the monodisperse droplets, it is necessary that the flow conditions are stable because any bubble or dirt can completely change the regime. In this way, any human fault during the device construction (misalignment, poor treatment of capillaries, dirt) could change the operability windows presented.. In this work, the production method of these devices was based on Michelon *et al.*[3]. In addition to reproducing them, it was also added another geometry to achieve different physical parameters. The devices used here are described in detail in section 3.3.2.

3.2.2 Production setup

Production of the double emulsion templates (O/W/O) was observed through an inverted microscope (DMi8, Leica Microsystem, Germany) using a high speed camera (Fastcam SA-3, Photron, USA), as shown in figure 3.7.

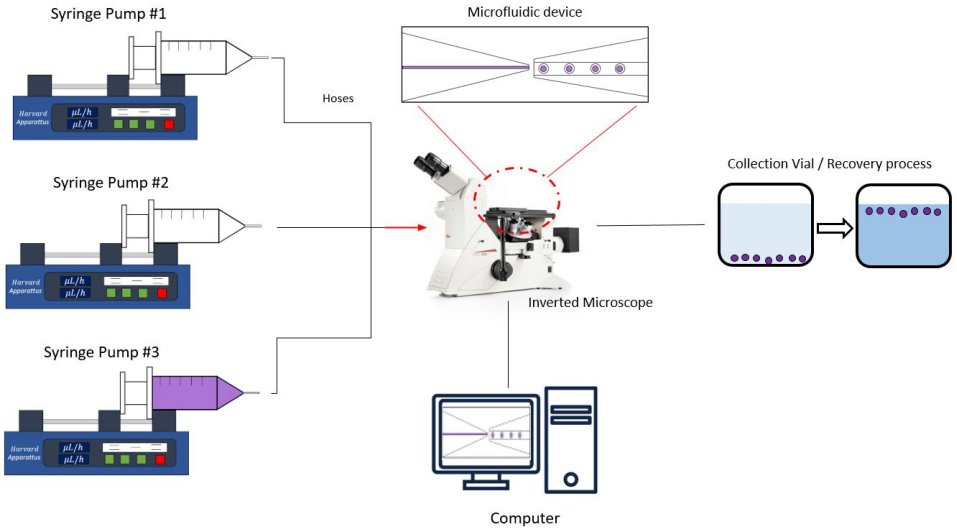

Figure 3.7: Production setup sketch.

Three syringe-pumps (Pump 11, Harvard Apparatus, USA) were used to control the flow rates of inner (Q_i), middle (Q_m) and outer (Q_o) phases. Three BD plastic syringes and four tubes, which three of them are connected with the dispensing needles of the syringe to the microfluidic device needles. Thus, the fluids flow first through these three connection tubes, then they saturate the device and finally flow through the last tube, connected with the collection capillary, reaching the recovery vial to collect the capsules. The tubes have 0.052" of outer and 0.034" of inner diameters and are flexible.

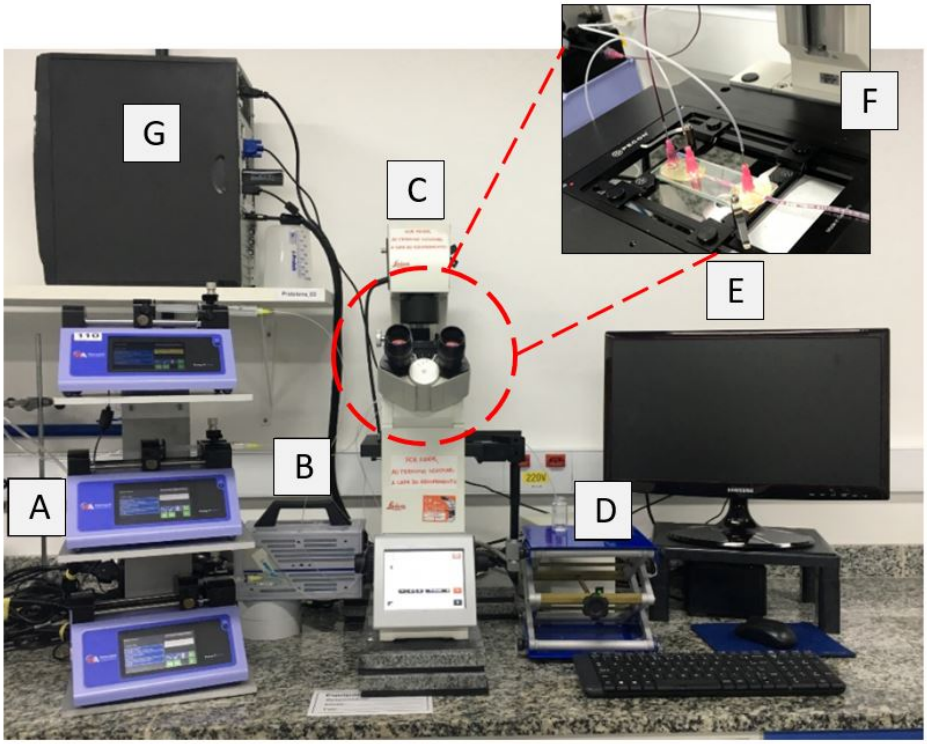

Figure 3.8: Production setup. (A) Three pumps with the three phases in the syringes. (B) camera. (C) inverted microscope. (D) collection vial with hexane. (E) Monitor. (F) Device under test. (G) Computer.

3.2.3 Collection

Michelon *et al.* [3] developed a recovery process using hexane to withdraw the remaining continuous phase of sunflower oil and then change to acetate buffer because many applications of the gellan gum microcapsules requires an aqueous capsular dispersion. Acetate buffer is an aqueous solution containing acetic acid and sodium acetate, ideal to stabalize gellan-based microcapsules [75]. Then, after gelification the previous O/W/O template turns into an O/W/W dispersion. However, if the application requires an oily system, the microcapsules could be collected in sunflower oil as well. This process of recovery is relevant due to a broaden application for the microcapsules because it enables them to be dispersed in hydrophobic and hydrophilic media. Figure 3.9 shows the capsules stabilized during the post-production collection process.

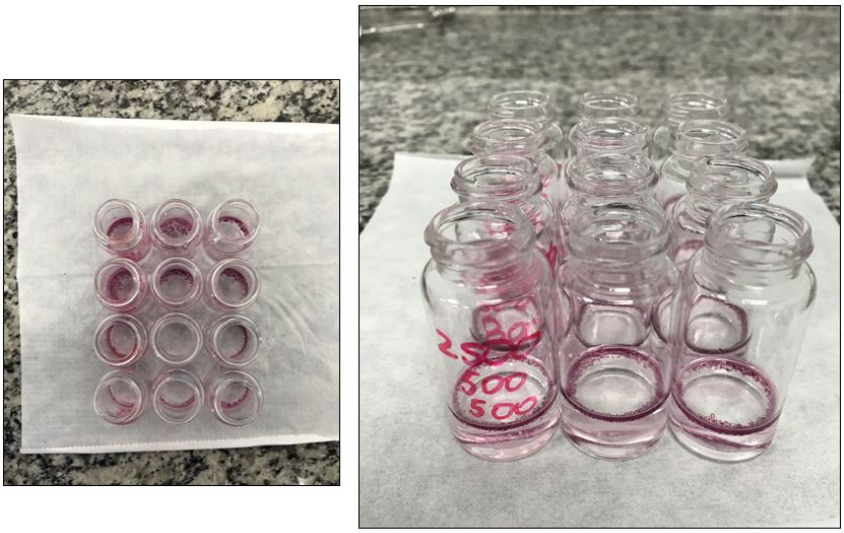

Figure 3.9: Post-production collection process. The capsules, in purple, produced are dispersed in acetate buffer.

3.3 Production

According to Michelon *et al.* [3] and Chen *et al.* [16], flow rates play an important role in the final characteristics of the microcapsules produced in microfluidic devices. The continuous phase flow rate (Q_o) is directly related to the size of the capsules, so the greater this flow, the smaller the diameter, also generating more capsules in less time. In addition, the thickness of its shell is related to the flow rates of the intermediate and internal phases. The ratio between them (Q_m/Q_i) will determine how thick your shell is, that is, the greater this ratio, the thicker it is and the more gellan is present in the composition.

To produce monodispersed droplets, a dripping regime, as shown in figure 3.10, is desired, which occurs when an absolute instability at which the viscous and capillary forces balance is such that both interfaces break simultaneously at the same spatial location and frequency. Therefore, we had to make a brief investigation of the operability window, varying the flow rates, which made this production possible.

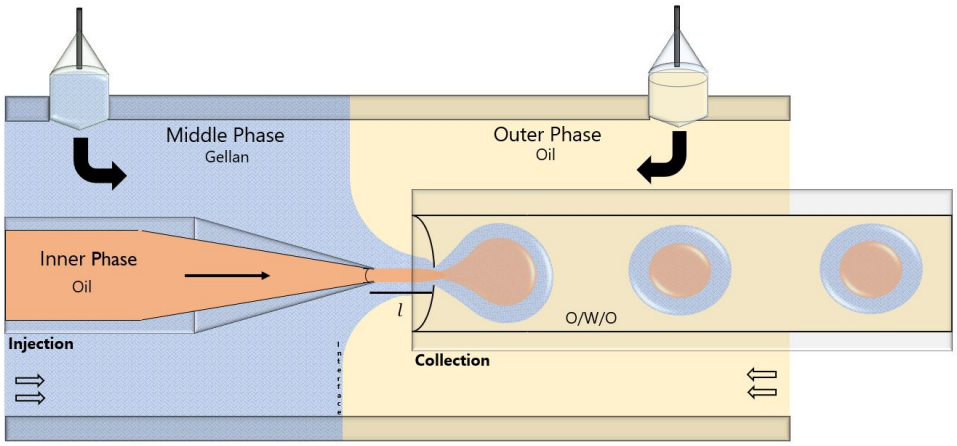

Figure 3.10: Detailed 2D diagram of the flow of liquids involved during the formation of double emulsions templates. The inner (orange) phase flows through the injection capillary while the intermediate (blue) and outer (yellow) phases flow through the square capillary until they meet on the tip of the collection capillary.

In this work different groups of microcapsules were produced and separated by diameter. Within these groups, shell thickness were varied in order to determinate how these properties affect the controlled release of the inner content of gellan gum microcapsules using temperature as the trigger mechanism.

3.3.1 Characterization

After production and recovery, every batch of microcapsules was characterized by their diameter and shell thickness. Figures 3.11 and 3.12 show the characterization process.

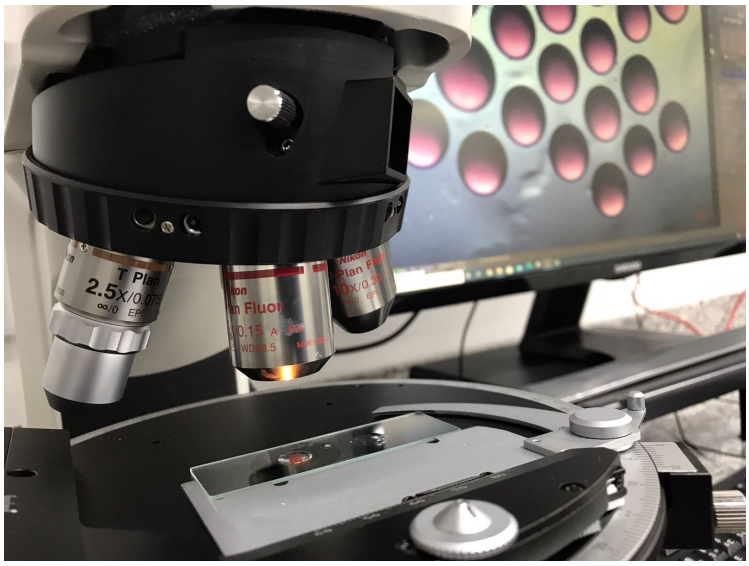

Figure 3.11: Nikon microscope used to perform sample characterization.

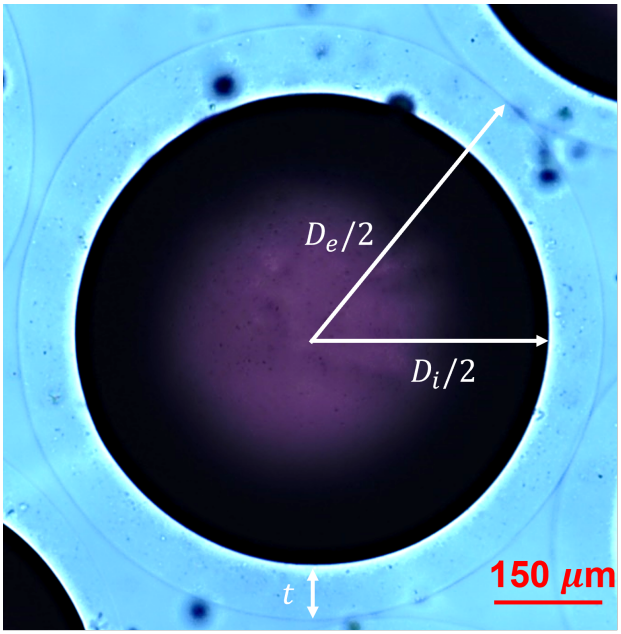

Figure 3.12: Detailed characterization of capsule diameter and thickness

The measurement of the capsule diameter and shell thickness was done using a microscope (Nikon Microscope ECLIPSE LV100POL, Japan) while the particles were dispersed in acetate buffer solution. The images of each individual capsule was processed using the software NIS Elements AR to evaluate the outer (D_e) and inner (D_i) diameters, as indicated in figure 3.12. At least 15 microcapsules were measured in each batch. Shell thickness was calculated from eq. 3-1:

$$t = \frac{D_e - D_i}{2} \tag{3-1}$$

3.3.2 Operability window

Besides the fluids composition, there are some important variables during microcapsules production that need to be controlled in order to achieve the desired conditions at which they can be properly fabricated. Once the device is at ideal production conditions, that is, aligned, treated, and cleaned, all that remains is to adjust the flow rate of each phase to reach the ideal regimes. Two different microfluidic devices were used to produce capsules of different sizes, as shown in table 3.2. The first was used to produce capsules of up to 250 μm, which we refer here as "small capsules", while the second served to obtain microcapsules ranging from 400 to 600 μm, classified as "large capsules".

Device	ϕ_i (μm)	ϕ_c (μm)	l (μm)
D-1	80	350	120
D-2	170	400	140

Table 3.2: Parameters of the designs used. Microfluidic device 1 (D-1) and microfluidic device 2 (D-2). D-1 and D-2 produced small and large capsules system, respectively

The effects of the flow rates of each phase on the O/W/O template generation for each of the two designs explored were investigated using three devices for each geometry. The ideal would be to use the same device to avoid any small variation in flow velocity associated with small differences in the geometry from device-to-device of the same design, but as they are disposable, it was much more feasible to use new microfluidic devices than to keep the same old one for a long time. The range of parameters at which the ideal intermittent dripping flow regime, as shown in figure 3.13, is based on the previous results by Michelon *et al.* [3]. However, along the way observed different regime, such as back-flow, when the outermost phase flow rate is much higher than the inner and middle phases, and jetting regime (figure 3.14), which produces microcapsules with higher standard deviations of its parameters.

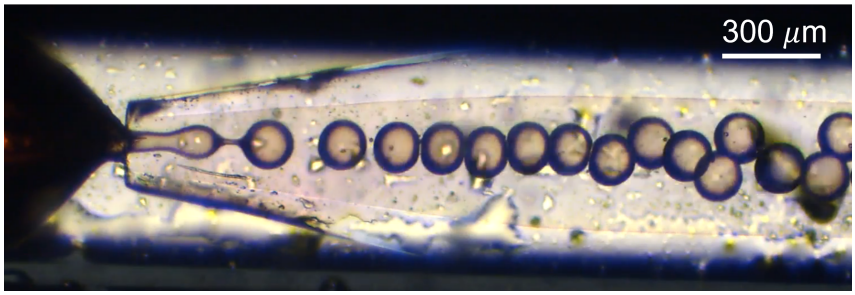

Figure 3.13: Desirable dripping regime with microfluidic device 1 (D-1).

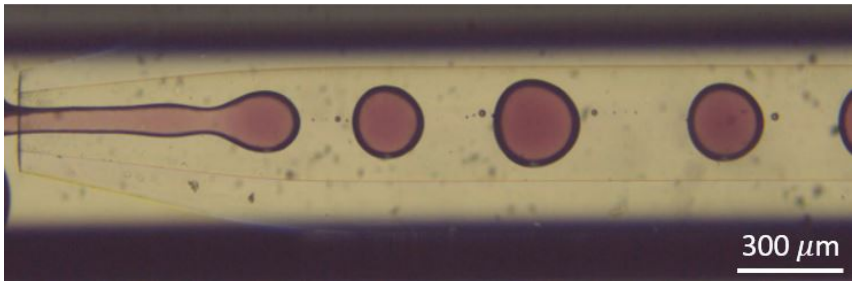

Figure 3.14: Undesirable jetting regime with microfluidic device 2 (D-2).

3.3.2.1 Microfluidic D-1: small microcapsules system

The results show that the capsule diameter can be reduced by decreasing the diameter of the tip of the capillaries and by increasing the outer phase flow rate. The shell thickness is varied by increasing the ratio between the middle and inner phase flow rate. Therefore, to analyze how the capsule dimensions affect the release time of the inner content by temperature trigger, it was necessary to produce groups of microcapsules separated by diameter and thus, for each one of them, vary the shell thickness as another parameter of comparison.

Microfluidic device 1 (D-1) can produce capsules of up to 300 μm. Based on Michelon *et al.* [3] and Leopercio's [7] work, we fixed the inner phase flow rate at at 200 $\mu l/h$. In this case, the flows of the intermediate and external phases are controlled in order to reach the desired thickness-diameter ratio (t/D). The shell thickness increases as the ratio Q_m/Q_i is increased. They also demonstrate that higher outer flow rates results in smaller diameters.

The micrograph, shown in figure 3.15, is an example of a result obtained after the procedure established for the production of the capsules. In addition to fixing the internal phase flow rate, we also selected a fixed outer flow rate of $Qo = 1500\mu l/h$. With the external and internal phase flows now fixed, in order to vary the shell thickness, we worked with middle phase flow rates between 25 and 300 $\mu l/h$.

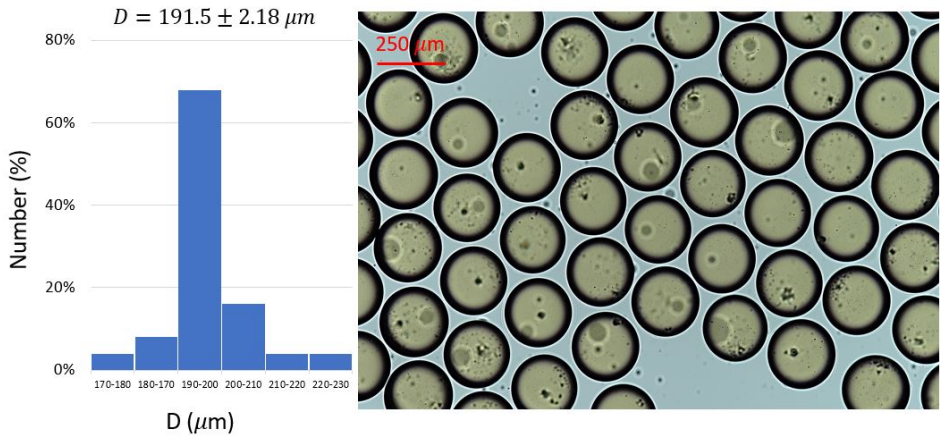

Figure 3.15: Micrographs with the characterization results after production of small capsules.

Notice that the diameter of this example is 191.5 μm, with a low standard deviation, showing the monodispersity achieved in the process. This result also showed that the parameters selected from previous studies [3, 7] fitted well to achieve the objective of producing small microcapsules.

As one of the objectives was to compare the delivery between "small" microcapsules, under the same thickness range, with a slight change in their size, we produced two groups, with the first being 15% larger than the second, as shown in the tables 3.3 and 3.4 below.

In section 4.3 of this dissertation, the "small microcapsules" produced were used to: find the optimal degradation temperature (can deliver all the internal content within the stipulated time), compare whether a slight change in size affects the degradation time (under the same thickness range) and compare them to the "large" microcapsules group produced with microfluidic device (D-2).

Sample	Diameter [μm]	Thickness [μm]	t/D [%]
1	220.2 ± 1.5	12.5 ± 1.3	5.7
2	223.8 ± 3.8	8.0 ± 1.8	3.6
3	221.5 ± 1.4	5.5 ± 2.1	2.5

Table 3.3: Group 1: $D \approx 221.8\ \mu m$.

Sample	Diameter [μm]	Thickness [μm]	t/D [%]
4	191.4 ± 2.2	11.5 ± 1.3	5.8
5	192.2 ± 2.5	6.1 ± 1.2	3.2
6	196.4 ± 4.2	4.3 ± 1.5	2.2

Table 3.4: Group 2: $D \approx 193.3\ \mu m$.

3.3.2.2
Microfluidic D-2: large microcapsules system

As previous microfluidic device (D-1) produced capsules with a maximum diameter of 300 μm, it was necessary to adapt its geometry to be able to generate larger capsules. The microfluidic device 2 (D-2) allowed the production of particles with sizes from 350 to 600 μm, larger diameter values than the microcapsules produced with D-1.

In order to achieve the best conditions of production, a sweep on the flow rate parameters had to be done for both types of gellan. Both were produced with the same weight percentage (0.5 wt%) but with different acyl percentage: 100% low-acyl, for the first, and 95% LA + 5% HA, for the second. Figure 3.16 presents the operability limits as a function of the outer and middle phase flow rates for the microfluidic device D-2 for the low-acyl (LA) gellan gum. The second operability window obtained for the high-acyl (HA) addition to the shell solution is shown in figure 3.17.

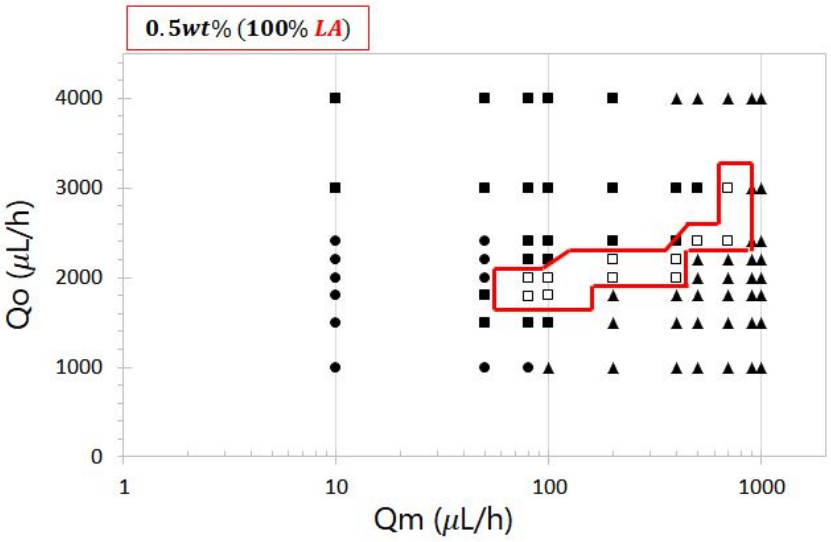

Figure 3.16: Operability window of production for the 0.5 wt% (100% low-acyl) gellan microcapsules. The red window represents the best conditions area of production, where the dripping regime is achievable

In the first window (figure 3.16), the internal phase flow rate was fixed at 700 $\mu l/h$. The filled circle (●) represents the back-flow regime, when the external phase flow overrun inner phase. The filled square (■) is the result of a simple emulsion formation, without inner content. The filled triangle (▲) shows the jetting regime, where droplets are formed far from the tip of the collection capillary, producing high standard deviation diameters. Finally, the ideal production regime is represented by the open square symbol (□), at

which the dripping regime was achieved and, consequently, capsules close to monodispersity were produced.

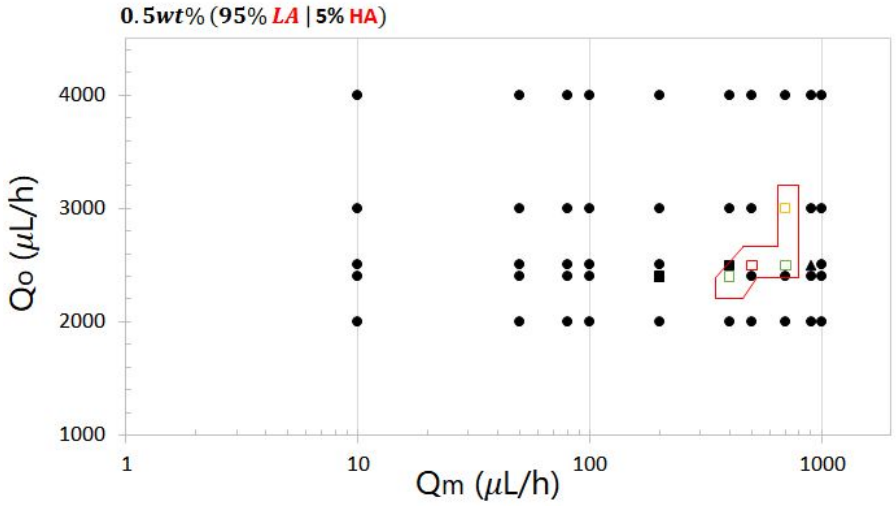

Figure 3.17: Operability window for production of the 0.5wt% (95% low-acyl + 5% high-acyl) gellan microcapsules. The red window represents the best conditions area of production, wherer the dripping regime is achievable.

The second operability window (figure 3.17), however, shows three different fixed inner flow rates (Q_i), represented by open squares with three different colors at the dripping regime region as follows: 400 $\mu l/h$ (□), 500 $\mu l/h$ (□), and 800 $\mu l/h$ (□). The production was done with the altered gellan mixture, with 95% composed of low acyl (LA) and 5% of high acyl (HA) gellan. As in the previous section, each symbol represents the same type of regime, the difference was in the adjustment of the inner phase flow to achieve the best conditions. The idea was to produce capsules with similar diameter and thickness, then compare the release time for different shell composition.

It is possible to observe in the graphs that the window to produce the capsules has decreased despite the same device geometry and flow condition. Thus, the chemical change in the composition of gellan, which changes the viscosity and interfacial tension of the middle phase may influence and, therefore, alter production regimes. Despite the modification, it was possible to produce capsules with the same geometrical characteristics.

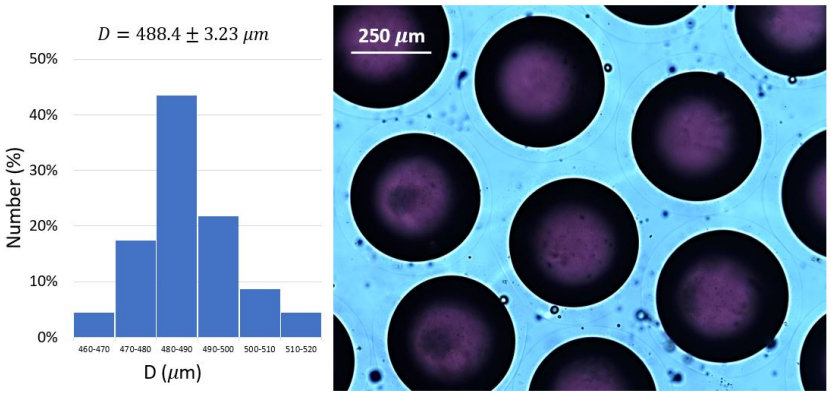

Figure 3.18: Micrograph with the characterization results after production of large capsules

Figure 3.18 shows an example in which we used micrographs to characterize the capsules of each sample. The diameters varied between 370 and 510 μm, while the flows rates explored are in the operability window shown previously on this section.

In the end, we produced two groups of "large" microcapsules, with thickness-diameter ratio of 4% to 10.3% . The first group (table 3.5) will be compared, in the next section, with the small microcapsules system and, furthermore, analyze how the shell thickness affects the inner content's release with fixed and variable temperature degrees.

Sample	Diameter $[\mu m]$	Thickness $[\mu m]$	t/D [%]
1	487.1 ± 42.8	50.4 ± 15.7	10.3
2	466.2 ± 30.9	34.2 ± 7.9	7.4
3	507.6 ± 27.3	21.9 ± 12.6	4.1

Table 3.5: Group 1 of large microcapsules (100% low-acyl) system produced with the microfluidic device 2 (D-2).

Sample	Diameter $[\mu m]$	Thickness $[\mu m]$	t/D [%]
1	488.3 ± 10.5	44.5 ± 3.2	9.1
2	450.3 ± 18.8	34.5 ± 6.2	7.7
3	463.4 ± 29.3	20.6 ± 4.4	4.4

Table 3.6: Group 2 of large microcapsules (95% low-acyl and 5% high-acyl) system produced with the microfluidic device 2 (D-2).

The second group (table 3.6) was produced with a chemical alteration in the shell composition, adding high-acyl (HA) to its structure. The goal was to compare the second group, with the same geometrical properties as group 1, regarding its sensibility to the heat rate involved.

The proposal to produce capsules based on the gellan biopolymer with different diameters and shell thickness was successfully achieved. The main parameter that changes the sizes is the flow rate of the continuous phase while the one that most affects the shell thickness is the flow rate of the middle phase (gellan). In addition, we were able to produce different gellan compositions, high-acyl and low-acyl.

4
Release Triggered by Temperature

As already mentioned in chapter 2, there are many mechanisms that can initiate changes in a capsule shell structure resulting in the release of its contents in this work, the focus is to study and understand the conditions under which a gellan-based biodegradable shell disintegrates by a thermal trigger event. Thermally induced release is useful in applications where changes in temperature naturally occur or can be easily imposed.

This chapter reports the degradation of suspended gellan-based microcapsules when exposed to higher temperatures. Gellan gum microcapsules, of different diameter and shell thickness, produced as described in the previous chapter, were used in the experiments. We discuss the effect of capsule properties on the dynamics of internal content release.

4.1
Experimental setup and methodology

The experimental setup used in this study is composed of a sealed support for the capsules, a heater, an inverted microscope, a controlled temperature bath, and a computer to acquire and process the images. Figure 4.1 shows a scheme of the experimental set-up for the controlled release under temperature stimulus.

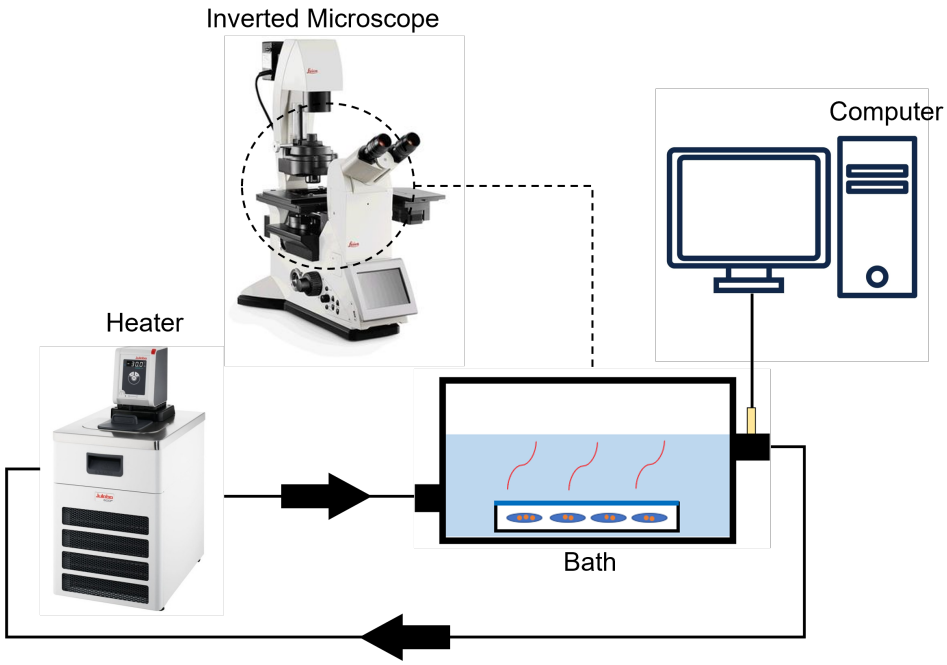

Figure 4.1: Scheme of the experimental set-up for temperature trigger event.

A kline's plate glass (10x7x2 cm, Qualividros Distribuidora LTDA) with twelve mini excavations of 1 ml each was used as a support to separate each sample of capsules distributed by their properties. Thus, the microcapsules are isolated from direct contact with the heating fluid. The sealing system, besides the kline's plate, is composed by the addition of grease on the surface of the support and silicone glue on its sides. The sealing is completed with a glass plate (10x7 cm) placed above the surface of the support and, finally, o-rings are added to increase the pressure on the glass in order to reduce the risk of leakage at the same time that the o-ring can withstand high temperatures. Figure 4.2 shows the kline's plate with the microcapsules inside.

Figure 4.2: Kline's plate with the printed (blue) support attached to it.

The kline's plate was placed inside a temperature controlled fluid bath. The bath (figure 4.3) was designed with the software Solidworks®, printed by a 3D printer (model SLA, Formlabs, USA) and an acrylic plate was designed and ordered to fit between the support and the bath, so that visualization could be done. In addition, the bath was designed with 2 o-ring sockets to prevent water from leaking out of the bath, both from below and above. Before fitting the 3 compartment's bath, it was necessary to place a layer of grease between the o-ring and the bath base/top, in order to guarantee the isolation of the fluid inside the entire structure. Soon after, the compartments are fixed with 14 screws of 10 cm each, crossing the entire assembled structure.

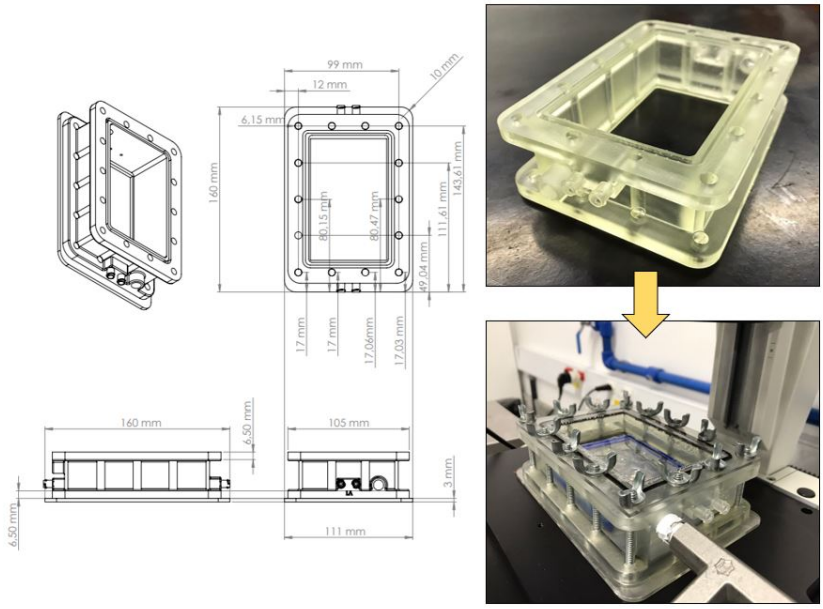

Figure 4.3: Detailed printed bath from its initial idea to its final form.

Temperature was measured by a thermocouple (National Instruments, USA, Model DR-4524) and the LabView®software was responsible for read and register the data. Finally, an inverted microscope (model DMi8, Leica Microsystem, Germany) was used for all visual part of the experiments and responsible for recording the tests. The software used was LAS X®. Figure 4.4 shows the setup used and each number is described in figure label.

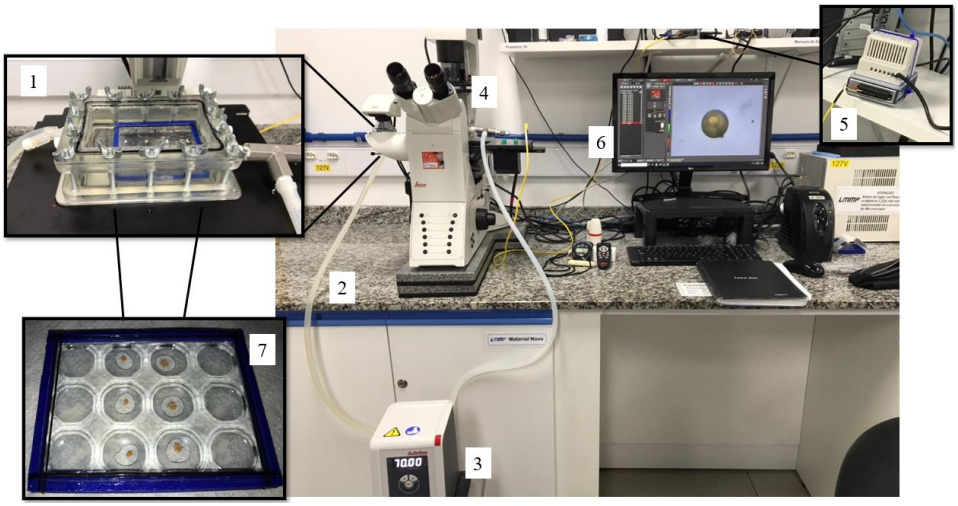

Figure 4.4: Experimental setup for the controlled release of gellan capsules.(1) bath, (2) hoses, (3) heater, (4) inverted microscope, (5) thermocouple, (6) computer, (7) kline's plate.

The vast majority of works in literature which studied temperature triggered release does not address gellan gum, and those who studied this

biopolymer do not use it as a protective capsule of its active, but rather as a substance for direct application, in the human body, for example [99]. Therefore, the shell destruction tests had to start based on the handling tests of gellan gum which is reported to dissolve in pure water at temperatures above 85 °C [4]. However, high acyl gellan gum forms a gel upon cooling from 65°C, while low acyl forms a gel upon cooling below 45°C [74]. Therefore, it was very important to know the temperatures that caused the gellan shell to deteriorate. Tests were divided with different temperature protocols.

4.2 Results and discussion

4.2.1 Heating protocols

As mentioned before, most of the literature dealing with gellan gum does not address this substance as a capsule and, in that it does, release triggers other than temperature are used [7]. Therefore, before any temperature selection for the tests, it was necessary to scan several temperature levels to find the region where the capsule's shell reacts to the heat stimuli and, from then on, define the ideal work temperature within the time window tested. The temperature protocols are listed and detailed below:

1. **Gradual increase:** Tests were carried out to find the ideal region at which the shell reacts to the stimuli of the environment. For this type of protocol, the experiment started at room temperature and ended when we found the temperature of reaction to the thermal trigger. As each temperature step involved more heat, we left the capsules under observation for longer periods under each temperature. That is, the higher the temperature, the longer the observation time. Figure 4.5 below shows a schematic representation of the temperature evolution during the test.

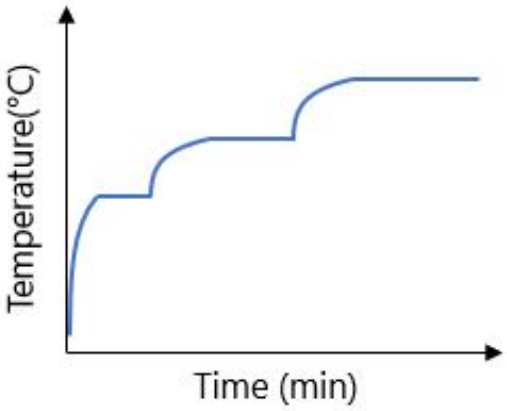

Figure 4.5: Gradual protocol.

In addition, this protocol was also used to evaluate how the heat rate increase can influence the release speed of the inner contents of the microcapsule.

2. **Fixed temperature:** This protocol was used in two ways. In the first one, several tests were carried out under fixed temperatures to find the one that guarantees the delivery of all the internal content of all the capsules within the elapsed time window. Figure 4.6 below shows an example of various fixed temperatures estabilished in order to find the ideal level that guarantees the delivery.

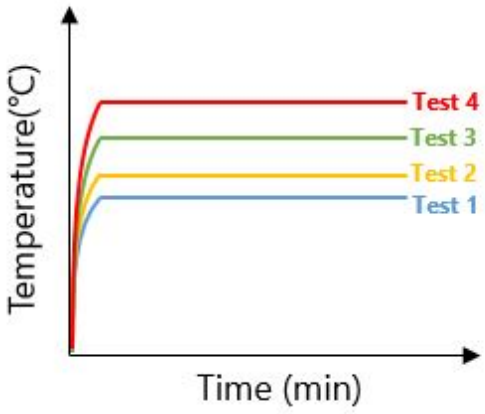

Figure 4.6: Fixed temperature protocol.

The second method is a consequence of the first one, at which we selected this optimal degradation temperature and, with it fixed in the tests from then on, we used it to perform comparisons between the relation of shell thickness (t) and capsule diameter (D) with the time of the release of internal content.

4.2.2 Quantification protocol

The quantification protocol to evaluate the evolution of the number of capsules that have not been destroyed was based on visual counting, with the Leica system, in which the inner phase releases were defined as a change in the color of the particles in the sample. This structure alteration occurred due to the change in the refractive index of the light incident into system.

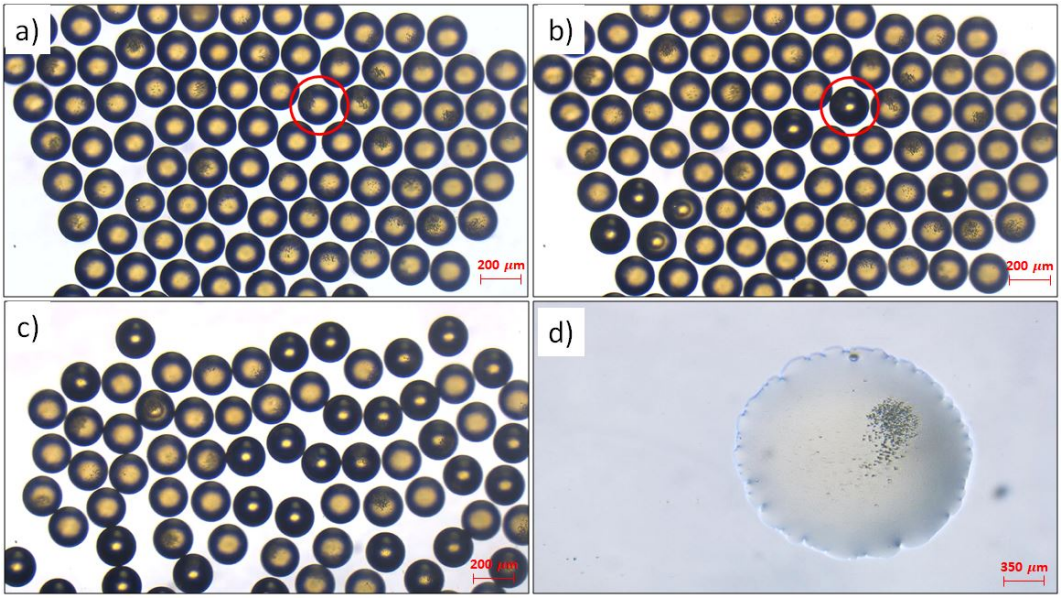

Figure 4.7: Quantification experiment at 75°C: a) Unaltered capsules in at the beginning of the test; b) Trigger reached and identified through the refraction index alteration (red circles); c) Trigger chain reaction leading to several deliveries; d) Oil coalescence post-trigger event.

Figure 4.7 represents an example from one of the samples with a complete historic view of capsules structure alteration, in (a) and (b) we can see how a single capsule structure clearly change from one stage to another. This change is observed when there is an alteration in the refractive index of the visualization. When the internal content is released, the structure becomes darker (circled in red). Then, in (c) we can see how many other capsules have also changed, losing its gellan gum shell. And finally, (d) represents the post-controlled release where oil drops are coalescing, a proof that there is no shell.

4.2.3
Optimum trigger temperature

In order to define the ideal temperature range at which the shell reacts to the temperature stimuli, we used the first protocol of gradual temperature increase. The test was focused on the capsule shell, without any type of quantification, just observing in detail the shell's reaction to the stimulus and thus finding the temperature region at which it is most sensitive. Table 4.1 shows the capsule sample used for the optimal temperature tests.

Sample	Diameter $[\mu m]$	Thickness $[\mu m]$	t/D [%]
4	191.4 ± 2.2	11.5 ± 1.3	5.8

Table 4.1: Physical properties used for optimal temperature trigger tests

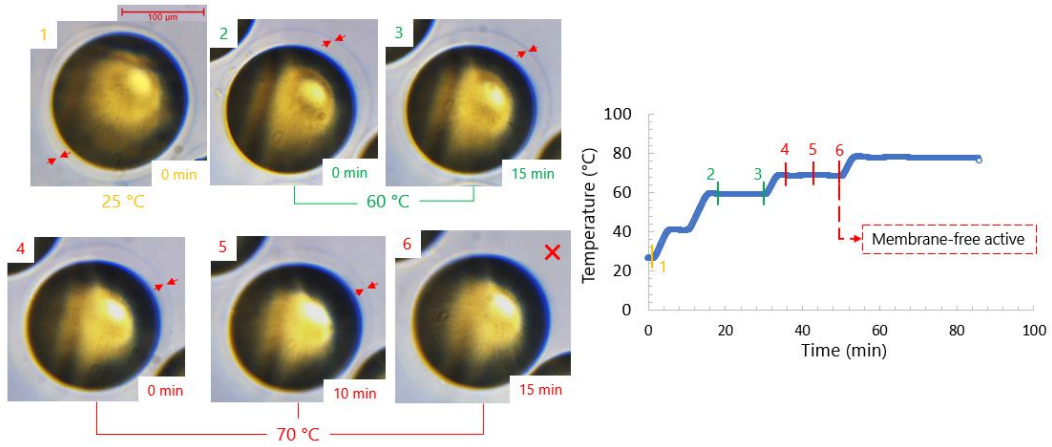

Figure 4.8: Gradual increase test; (1) Original capsule at room temperatuere. (2-3) At 60°C the membrane is still intact with few modification in its eccentricity. (4-5) 10 minutes at 70°C with the shell still observed. (6) After 15 min, the shell wall no longer exists.

The 20x zoom lens of the Leica® provided the visualization focused only on the behavior of the capsule's membrane.

As figure 4.8 shows, the first changes starts at 60 °C (2), changing the capsule's eccentricity. Increasing the temperature level to 70 °C it is observed that, within 15 minutes, the membrane no longer exists (6). The shell disappearance should be an indicator that the trigger for its degradation is in the range of 70 °C. As this verification was done with single capsules, it was necessary to reduce the working lens for observation of the evolution of a large group of capsules. As already mentioned in chapter 2, there are several

kinds of degradation and the discussion about them involving the gellan shell will be addressed later this chapter.

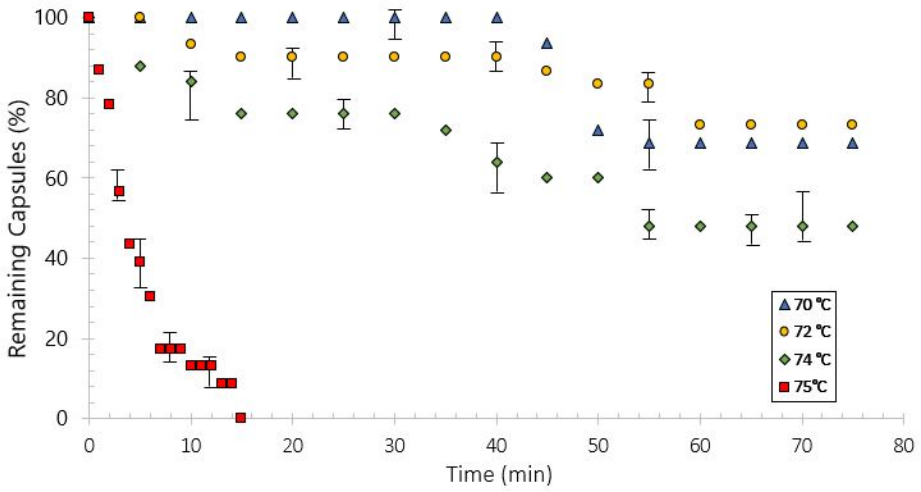

Figure 4.9: Remaining capsules for differentt temperature levels. 70 < T < 74 °C were not capable of full shell destruction; At 75 °C there is an abrupt drop with the remaining capsules.

After determining the temperature range for the capsule shell rupture, the trigger activation procedure was changed to the fixed temperature protocol. To compare the differences between each imposed temperature level, we analyze the release of the inner content of the microcapsules with the characteristics presented in table 4.1. Samples containing approximately 40 capsules were heated to different temperature levels. Figure 4.9 shows the number of remaining capsules as a function of time for different set temperatures.

- $T < 70°C$: Most of the microcapsules remained intact, without release;
- $T = 70°C$: The first releases were observed after 45 minutes. At the end of the window test, after 80 minutes, approximately 75% of the capsules remained intact;
- $T = 72°C$: This temperature proved to be efficient for trigger response, accelerating release. Within 15 minutes we observed the first releases of the content. However, this temperature was not enough to increase the number of capsules degraded under the same time window in relation to the previous temperature;
- $T = 74°C$: Once again the reaction speed at the beginning of the test increased, and this temperature was enough to decrease the number of capsules remaining to 48%;

– $T = 75°C$: In less than 2 minutes, the capsules already responded to the trigger and, within 15 minutes, there were no more capsules left in the sample.

One of the possibles reasons that could explain this controlled release is the polymer hydrolysis [100] in which, at a specific temperature level under acidic conditions, produces monosaccharides by breaking the glycosidic links between the monomer units in the structure of the molecule. These glycosidic links were formed during gelation of the gellan-based shell through the crosslinking process, as already mentioned in chapter 2. One of the most susceptible methods to break the bond is through hydrolysis reaction [1], triggered by the temperature stimuli added to the acidic medium at which it is inserted. The continuous phase at which the capsules were suspended in our tests is an acidic acetate buffer mean, pH=4.5. Preliminary tests with saline water showed that, under the same temperature levels, the gellan shell did not change. Thus, the pH conditions were changed to equalize acetate's, and yet the microcapsules did not deteriorate. This resistance may be related to the strong ionic bonds that support the gellan and saline water interface, reinforcing the crosslink.

Controlled release by temperature trigger is evident at 75°C with the quick response to the stimulus generating a total degradation of the samples within 15 minutes. So, we selected this level as the optimal temperature trigger (OT), being a threshold between a complete and a partial release, under 80 minutes elapsed time window. Thus, this OT proved to be more viable for the contents total release, acting as an instant stimulus under these conditions.

4.2.4 Properties comparison

Now that an optimal temperature trigger to degradation of gellan capsules has been established, the particles were manipulated by size and shell thickness to analyze how different properties influence on the thermal trigger response. The temperature method used will be the fixed temperature protocol at 75°C and we used the produced samples of microcapsules from chapter 3 to analyze the inner contents release. The quantification of the percentage number of the remaining intact capsules throughout the tests was based on frame analysis of the recorded videos by Leica System®. In each sample, the average amount of microcapsules was 50 particles per test.

4.2.4.1 Small capsules system: D $<$ 250 μm

The microcapsules used in this section are shown in tables 4.2 and 4.3.

Sample	Diameter [μm]	Thickness [μm]	t/D [%]
1	220.2 ± 1.5	12.5 ± 1.3	5.7
2	223.8 ± 3.8	8.0 ± 1.8	3.6
3	221.5 ± 1.4	5.5 ± 2.1	2.5

Table 4.2: Small microcapsules system - Group 1: $D \approx 221.8\ \mu m$.

Sample	Diameter [μm]	Thickness [μm]	t/D [%]
4	191.4 ± 2.2	11.5 ± 1.3	5.8
5	192.2 ± 2.5	6.1 ± 1.2	3.2
6	196.4 ± 4.2	4.3 ± 1.5	2.2

Table 4.3: Small microcapsules system - Group 2: $D \approx 193.3\ \mu m$.

The capsules are divided into two size groups, where capsules from group 1 is 15% bigger than group 2, but within them, the same shell thickness-diameter ratio (t/D) range aiming to analyze how this properties affects the inner content's release behavior for the same thickness values for different sizes.

After data analysis, we registered few differences between the two groups. Figure 4.10 presents the evolution of the number of capsules that had released its content from group 1 ($D \approx 221.8\mu m$). The sample with capsules with thinner shell ($t/D = 2.5\%$) had all the capsules destroyed after approximately 6 minutes. This time increased as the shell thickness increased. The sample with capsules with $t/D = 5.7\%$ had all the capsules destroyed after approximately 10 minutes.

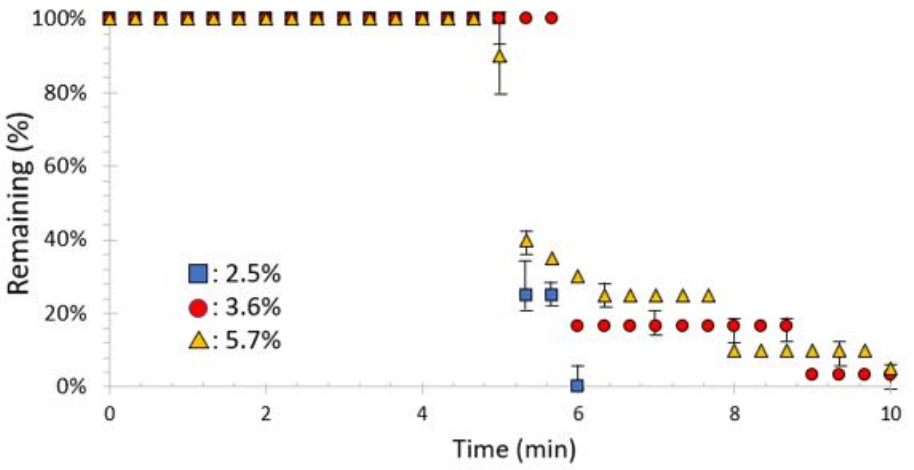

Figure 4.10: Evolution of the number of capsules remaining group 1 ($D \approx 221.8\mu m$) with an average release time of 8.7 minutes.

The degradation behavior of group 2 ($D \approx 193.3\mu m$), presented in figure 4.11, have a similar evolution as group 1. Thinner shell ($t/D = 2.5\%$) once again presents a faster release, while thicker ($t/D = 5.8\%$) slow down the release rate.

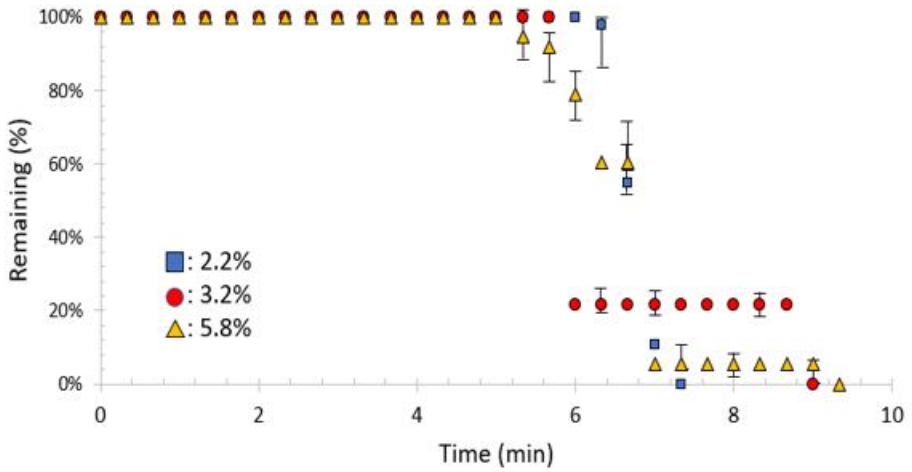

Figure 4.11: Evolution of the number of capsules remaining group 2 ($D \approx 193.3\mu m$) with an average release time of 8.4 minutes.

The results found for the small capsules system showed that both groups behave in a similar way. Microcapsules with the smallest t-D ratio ($t/D = 2.5\%$) delivered its inner content faster than the largest ($t/D = 5.8\%$) ratio, indicating that there is an influence of gellan percentage on the controlled release physics. Although the release times are different, they are very close to each other, which could also be explained by the experimental uncertainty of the test. In order to enhance this investigation, another group classified as "large" were studied and compared as shown in the next sucsection.

4.2.4.2 Large capsules system: 400 < D < 520 μm

To better understand the influence of the propreties os the microcapsules on the trigger activation event, it was necessary to produce microcapsules with larger diameter and shell thickness than those studied in the previous section. Table 4.4. presents the dimensions of the capsules used in these tests. As the size of the particles increases, so does their mass and the total shell degradation time would be expected to also increase. Furthermore, the shell thickness concerning its diameter was also increased, we managed to double the thickness-diameter ratio (t/D) from the small capsules system.

Sample	Diameter [μm]	Thickness [μm]	t/D [%]
1	487.1 ± 42.8	50.4 ± 15.7	10.3
2	466.2 ± 30.9	34.2 ± 7.9	7.4
3	507.6 ± 27.3	21.9 ± 12.6	4.5

Table 4.4: Bigger capsules produced with the microfluidic device 2 (D-2).

Size comparison is a promising lead that physical parameters do matter the heat transfer process that takes place and to the gellan gum dissolution. Figure 4.12 shows one example of test with these new proprieties :

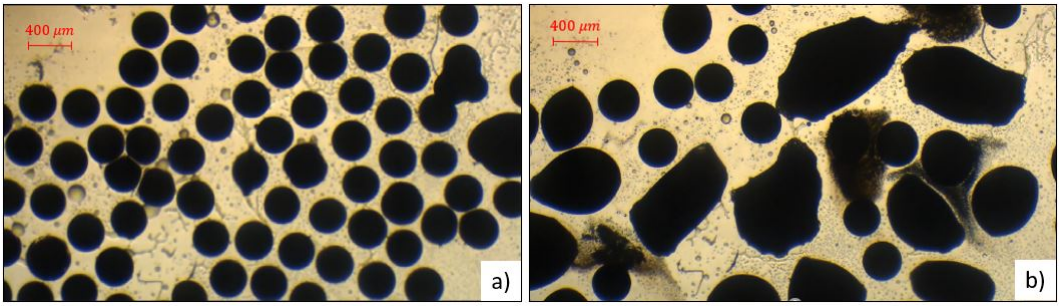

Figure 4.12: Behavior example after 40 minutes of test from the large microcapsules system group (D= 508 μm, t/D= 4.5%). a) Original structure at room temperature. b) Test after 40 minutes at 75°C.

As in the previous section, the tests were performed with the fixed temperature protocol at 75°C . Figure 4.13 shows the influence that shell thickness has on release time. Four tests were performed per size, and each point is the result of the average release number.

Figure 4.13 shows the evolution of the number of remaining capsules within a 90 minutes window time test. We noticed that the first big difference is in the degradation time:

- The small capsules system ($D < 250\mu m$) had an average release time of the actives lower than 10 minutes;
- The large capsules system time, required to delivery all inner content, is in the range from 40 minutes (thinner shells: t/D= 4.5%) to 70 minutes (thicker shells: t/D= 10.3%);
- This difference represents a 300% to 600% increase in time required compared to the small capsules system.

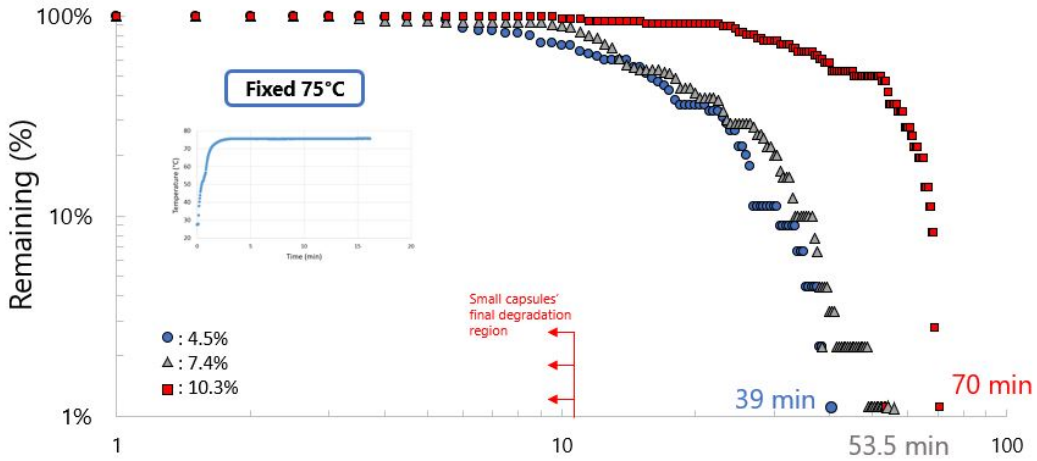

Figure 4.13: Evolution of the number of remaining large microcapsules system within 90 minutes operability window for several thickness steps under the fixed temperature protocol.

Furthermore, we can see the clear difference that each level of thickness exerts on the response to the trigger:

- Samples 3 (D=507 μm, t/D=4.5%) and 2 (D=466.2 um μm, t/D=7.4%) despite having a similar behavior, they have different times at the end of the degradation of 39 and 53.5 minutes, respectively;
- Sample 1 (D=487.1 μm, t/D=10.3%) shows the biggest difference within the system. In addition to having a slower stimulus response, it also has the longest time, 70 minutes, required to deliver all loaded actives.

Unlike the previous section, larger and thicker capsules have a greater tendency towards temperature resistance. This could be explained by the greater mass present both in the total particle diameter (internal phase plus shell) and the membrane alone. That is, the thicker the shell is, the longer time/heat will be required to completely degrade the microcapsules.

4.2.4.3 Heat rate increase

One way to try to accelerate the release time is to change the outer environment temperature. We study the dynamics of the system as the temperature was increased above 75 °C. So, the temperature control method changed from fixed temperature to gradual increase protocol, as shown in figure 4.14.

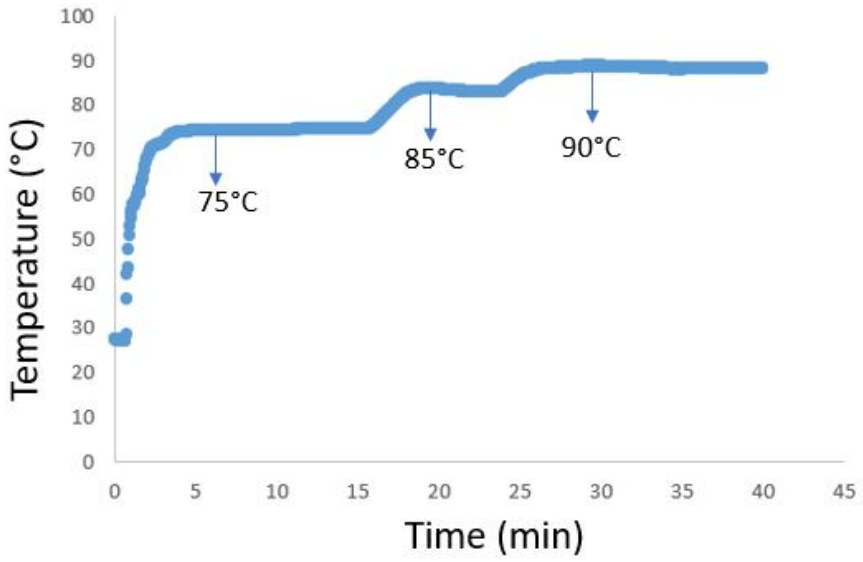

Figure 4.14: Heat rate increase protocol.

The idea is to start at the OT temperature (75°C) and increase it after a pre-setted period. We selected the increases to 85°C at 15 minutes and 90°C at 22 minutes, as shown in figure 4.15. These two time points were selected because, in the fixed temperature tests, this was the region that had few releases compared to the entire test. Therefore raising the temperature level in this period was a viable option in order to investigate the new evolution of the release under a transient regime.

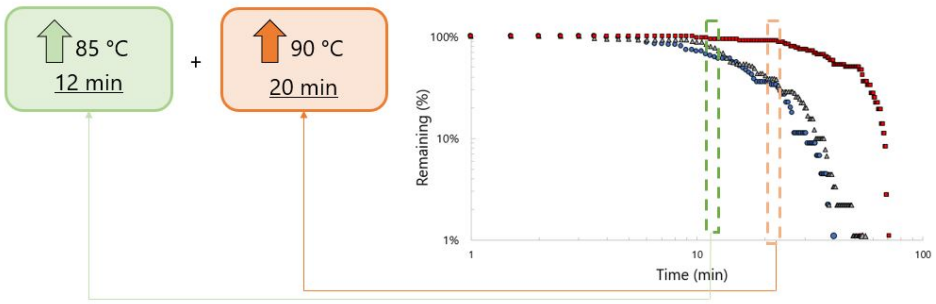

Figure 4.15: Time choice for temperature modification and the consequent increase in heat rate involved in the process.

The results were divided into 3 parts and performed with the same system of large capsules presented in table 4.4. The comparison was made by thickness-diameter ratio.

The comparison between the behavior of the original test (fixed temperature at 75°C), in dark blue, and the modified one (heat rate increase), in light blue, is shown in figures 4.16, 4.17, 4.18. Figure 4.16 compares the lowest

system thickness ratio (D=507.6,t/D=4.5%) where the degradation evolution is similar at the beginning and in the middle of the test. However:

- The original test released all its inner contents within 39 minutes;
- The heat release protocol accelerated the release, degrading all capsules within 36 minutes;
- Although it only reduced the total time by 7.69%, it is an indication that the temperature increase influenced the temperature trigger response

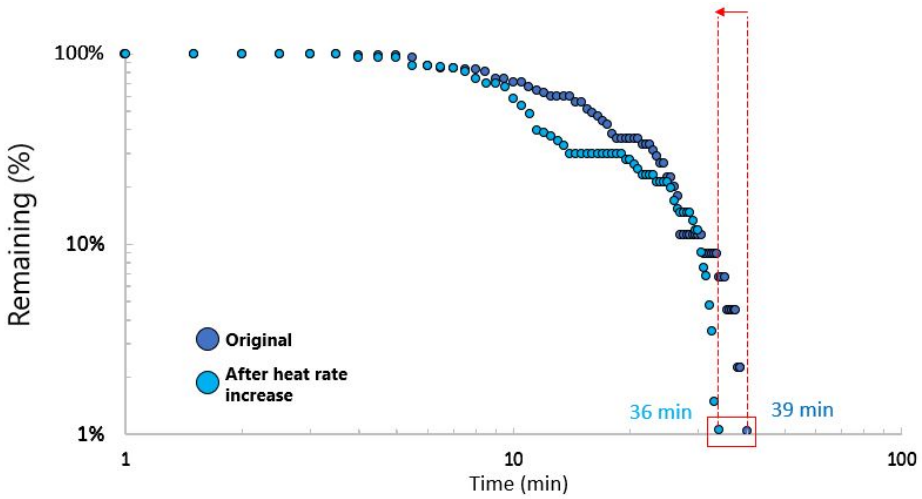

Figure 4.16: Comparison of the degradation evolution of thin shell microcapsules (t/D=4.5%) between the temperature increase (light blue) and fixed temperature (blue) protocols.

The investigation continued for the system sample with the intermediate t/D ratio (D=466.2,t/D=7.4%), as shown in Figure 4.17, and we concluded:

- The release dynamics changes only near the end of the test, for t $>$ 30 min.;
- While the original test took 53.5 minutes for complete release, the heat rate increased temperature test took 36.5 minutes;
- There is a 31.80% reduction in degradation time increasing the heat rate.

In this case, we already see a greater percentage of reduction in comparison to the first sample.

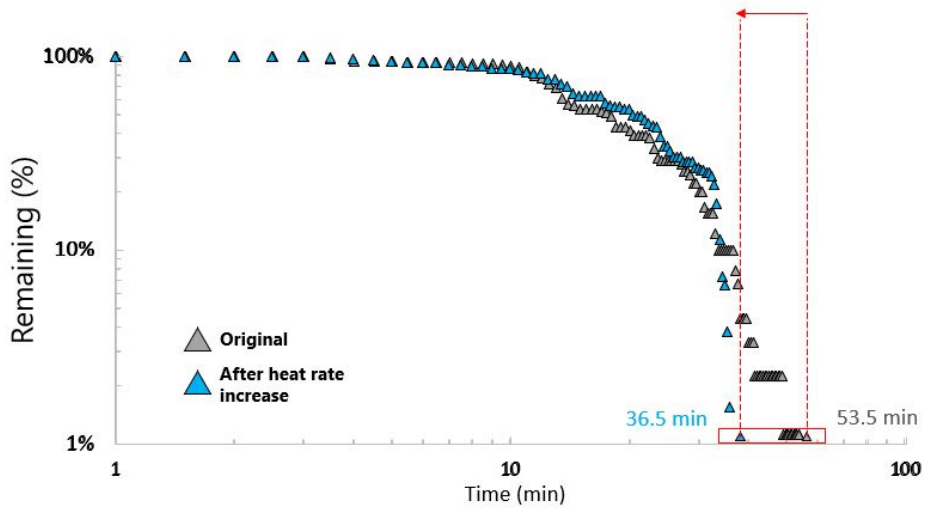

Figure 4.17: Comparison of the degradation evolution with thicknes/diameter ratio of 7.4% between the temperature increase (light blue) and fixed temperature (gray) protocols.

Finally, as shown in figure 4.18, we ended up with the test of the greater thickness of the system (D=487.1,t/D=10.3%):

- Unlike the other two cases, the behavior was shifted and modified from start to finish, showing a greater sensitivity of response to the higher imposed temperature levels;
- While the original test lasted about 70 minutes, the heat rate increase protocol reduced to 40 minutes;
- This half-hour decrease represents a 42.9% shorter time when working with higher temperatures concerning its optimal degradation temperature.

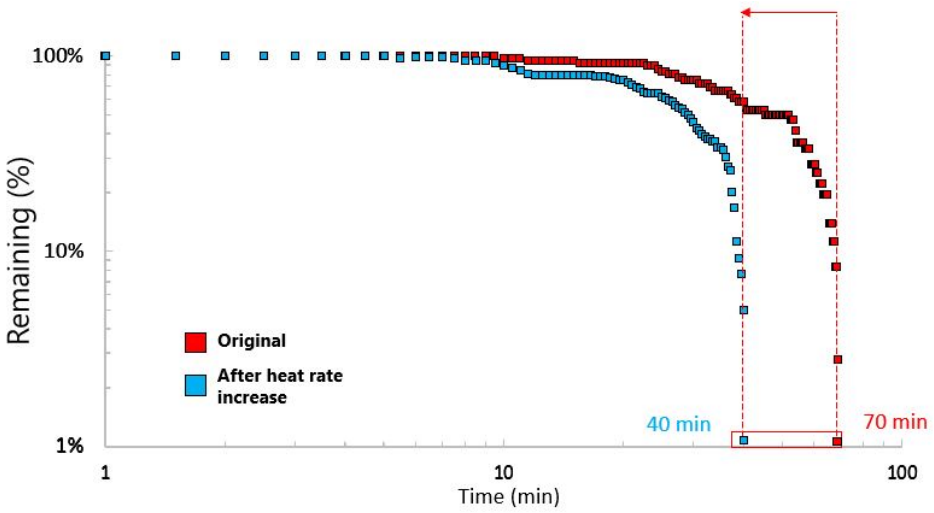

Figure 4.18: Comparison of the degradation evolution of the thicker shell microcapsules (t/D=10.3%) between the temperature increase (light blue) and fixed temperature (red) protocols.

Table 4.5 below summarizes the time reduction results when the new transient temperature regime is imposed on the system. In it, it is verified that the percentages of reduction increase as the thickness of the shell increases. This increase may be related to the greater contact surface between the shell and the bulk. Furthermore, as there is a higher percentage of gellan in the microcapsule structure, it is possible that there are more weak points in the crosslink bonds formed during the gelation process.

Sample	t/D [%]	Time reduction [%]
3	4.5	7.7
2	7.4	31.8
1	10.3	42.9

Table 4.5: Relation of the test time decrease between the constant temperature method (75°C) and the gradual increase (75 to 90°C). The second method involves a higher heat rate involved.

The above tests showed that the more percentage of gellan the microcapsules have, the more they are sensitive to the new transient temperature increase regime. Figure 4.19 below shows all the results summarized where one can find specific time releases from the first until the last reaction for each type of protocol and physical propertiesof the microcapsules.

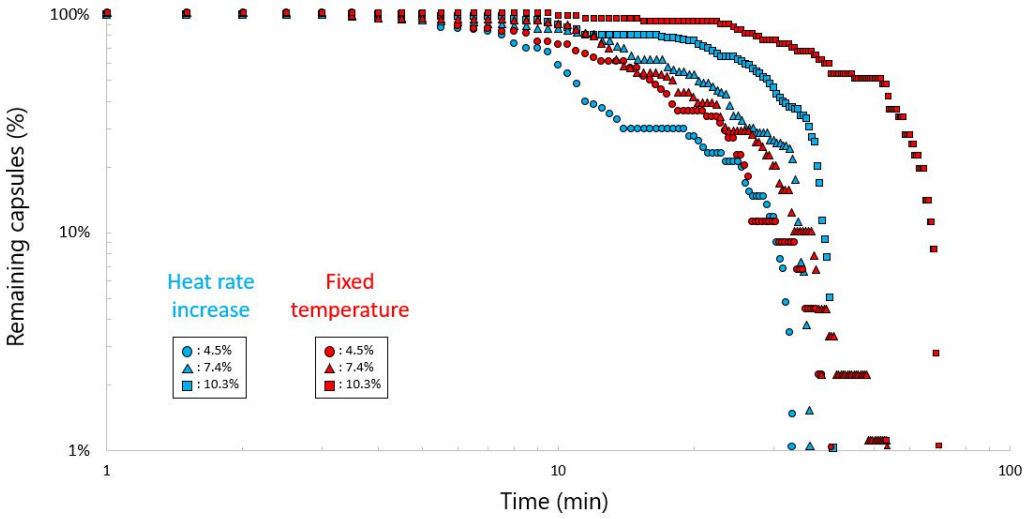

Figure 4.19: Degradation evolution for the large microcapsules system with fixed temperature (red) and heat rate increase (light blue).

4.2.5 High-acyl gellan addition

Previous research findings related to gellan form stated that low-acyl (LA) gum was found to be more stable than mixtures with low/high acyl gellan gum blends and the higher the percent of high acyl gellan (HA) gum, the more rapidly the gels degraded, producing weaker gels [101].R. Mao *et al.* [4] also studied the strength, deformability, and firmness of the gellan forms stating that the mixed gels, HA and LA, were much more deformable with similar strengths but yet weaker than LA gels.

Unlike previous findings, this work studies the application of gellan-based microcapsules under temperature influence leading to a series of degradation levels, depending on the temperature protocol imposed to the system and the physical properties of the capsules

In the previous experiments in this work, we used the gellan composition of 0.5 wt% with 100% of its low acyl (LA) form. In this current section, a solution alteration in the polymer chain was done, adding a new property to the mixture with the high-acyl (HA) gellan gum form. For this, the marble form of the composition will still be based on the low-acyl form, as shown in table 4.4, but adding a low concentration of the high-acyl form.

As mentioned in section 4, modified gellan microcapsules (95% LA - 5% HA) were produced to resemble the 100% LA capsules both in size and shell thickness. Table 4.6 above shows the samples produced. The idea was

Sample	Diameter $[\mu m]$	Thickness $[\mu m]$	t/D [%]
1	488.3 ± 10.5	44.5 ± 3.2	9.1
2	450.3 ± 18.8	34.5 ± 6.2	7.7
3	463.4 ± 29.3	20.6 ± 4.4	4.4

Table 4.6: Physical properties of gellan-based microcapsules (0.5wt%) composed with 95% low-acyl and 5% high-acyl.

to produce capsules with the same physical properties as group 1 of the large microcapsules system table 4.4 but with different chemical composition.

Preliminary viscosity and compression tests were performed in order to compare the difference between the new gellan composition (95% LA + 5%HA) with the 100% LA. The idea was to show that structurally, for this new composition, there are no major differences between the two and that the difference in the results of the temperature trigger tests to evaluate the release of actives from the new microcapsules may be related to the chemistry of its composition and, a result that will be shown below, can influence the desired type of application for different gellan microcapsules.

Then, before begining the temperature trigger event, we measured the viscosity as a function of temperature. The objective was to evaluate if the viscosity of both gellan mixtures would be different under the influence of the heat rate increase. Figure 4.20 below shows that the behavior is the same for both mixtures, with a slight lag at 70 °C. Thus, viscosity is not a determining factor that could explain a possible behavior alteration under the temperature trigger event for both types of gellan-based microcapsules.

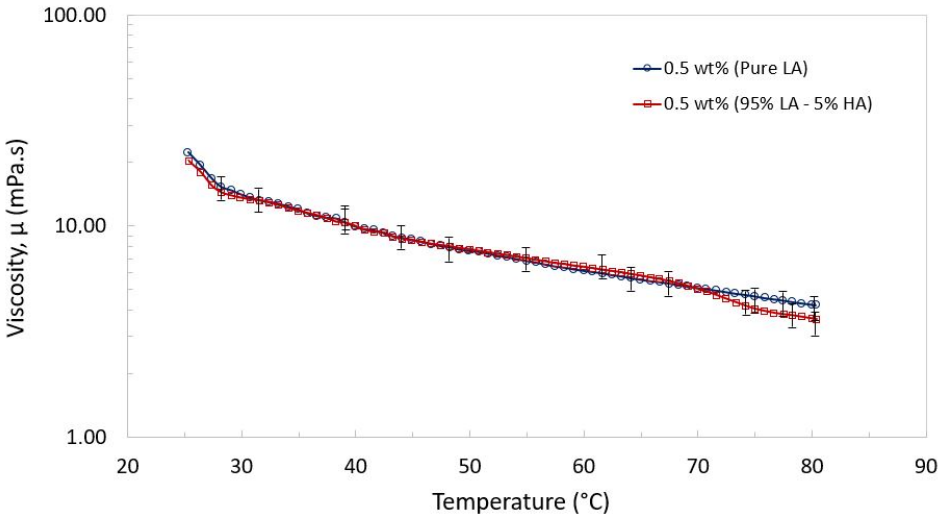

Figure 4.20: Viscosity behavior as a function of temperature.

Furthermore, to investigate possible structural differences of the two gellan mixtures, we performed compression tests on the rotational rheometer

(model DHR-3, TA Instruments, USA). These tests were performed with gelled gellan specimens, not with microcapsules, as shown in figure 4.21. The gelling of the liquid gellan mixture was carried out by adding an aqueous solution of calcium acetate (1wt%) to the mixture, to crosslink the covalent bonds formed and thus form the crosslink bonds, then gelling the gellan mixture. Once gelled, our specimen was ready.

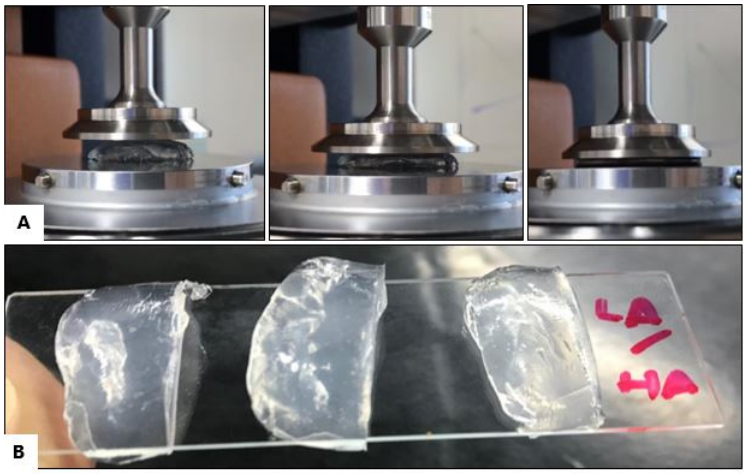

Figure 4.21: Compression test on rotational rheometer (A) and examples of gellan gelified speciemans (B).

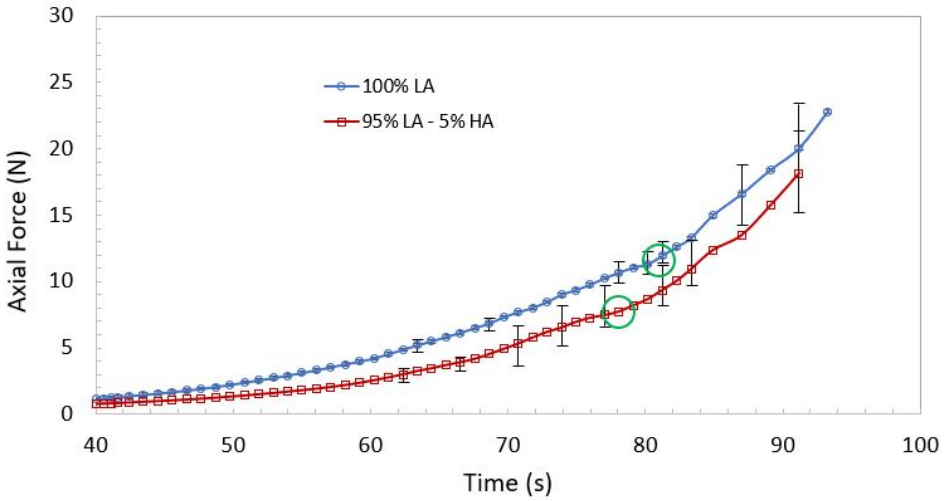

Figure 4.22: Compression force behavior for the two types of gellan used in the microcapsule shell.

As shown in figure 4.22 the compression test was performed for 100 seconds. The rupture of the specimen occurred in the green circles, and the result corroborates previous studies that state that a mixture of gellan with the high-acyl chain in its composition (95% LA + 5% HA) is weaker [4, 75].

According to our test, it is necessary to have a lower compression force to be able to break the specimen.

4.2.5.1
Optimum trigger temperature with high-acyl addition

As in section 4.2.3, we mirror the fixed temperature protocol in order to find the optimal trigger temperature for this new gellan. Figure 4.23 shows the results of the tests, with capsules of diameter 463.4 μm and t/D ratio of 4.4%, which the ideal temperature level for the inner contents full release is at 75°C. Lower levels proved to be ineffective in releasing the internal content. As with the results of section 4.2.1, the behavior was very similar in which the higher the temperature, the faster the shell deteriorates. As we increase the temperature level, fewer capsules remain. In addition, we have the comparison of degradation times for this same test with the 100% LA capsules (in black circles), and we see that the time required for the complete release of the content is shorter for the new capsules (95%LA + 5% HA) with the lower thickness-to-diameter ratio (D=464.4, t/D=4.4%) for this new system of microcapsules.

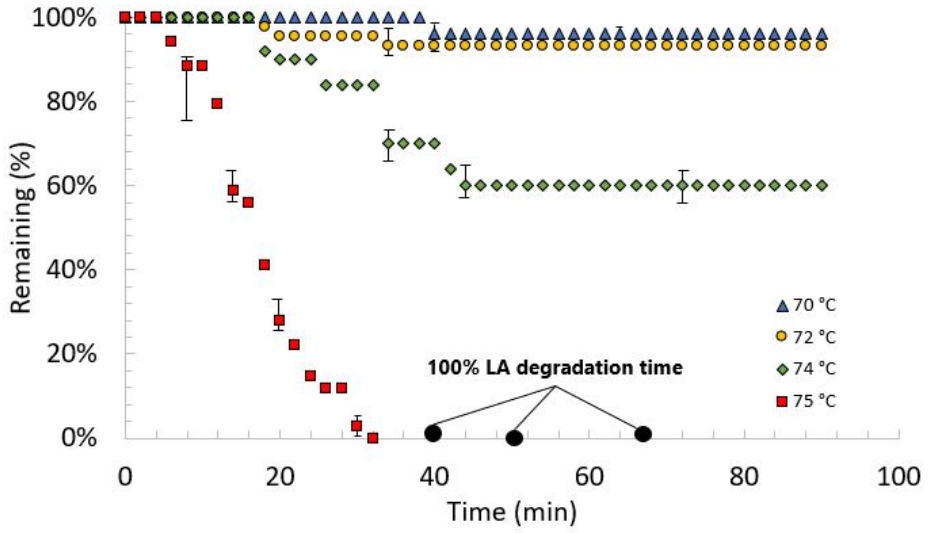

Figure 4.23: Fixed temperatures protocol test for the new microcapsules system with high acyl addition showing the evaluation of the remaining particles under temperature inffluence.

4.2.5.2
Heat rate increase with high-acyl addition

The method used to compare both types of gellan was the heat rate protocol, starting at OT temperature (75°C), rising to 85°C and ending at

90°C. The comparison was performed for each thickness level. It is worth remembering that the new capsules, with the addition of high-acyl, were produced to have the same physical properties as the "large" microcapsule system of section 4.2.4.2. Figures 4.24 and 4.25 show the degradation evolution under temperature trigger event in comparison to the original system of 100% LA gellan capsules. The yellow symbols represent the microcapsule with the addition of high-acyl, while the blue symbols represent the original microcapsule system.

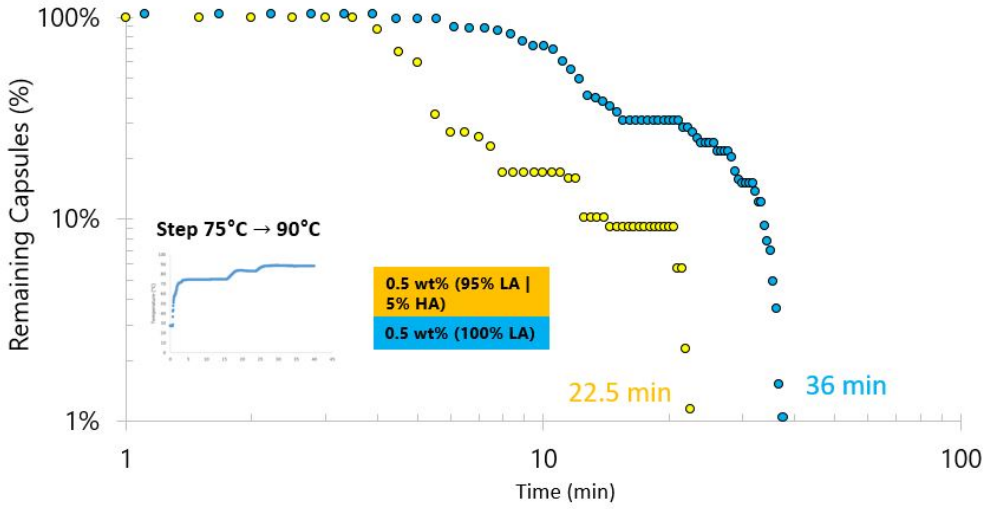

Figure 4.24: Evolution of microcapsule degradation under the heat rate increase protocol for thinner shell (D=463.4 μm, t/D=4.4%).

Figure 4.24 shows the evolution of the controlled release for the thinner microcapsules (D=463.4 μm, t/D=4.4%). Comparing the curves, we can see that:

- The altered gellan microcapsules were triggered faster;
- The total time required for its full release was 22.5 minutes;
- There is an indication that the altered microcapsules are more sensitive to the heat;

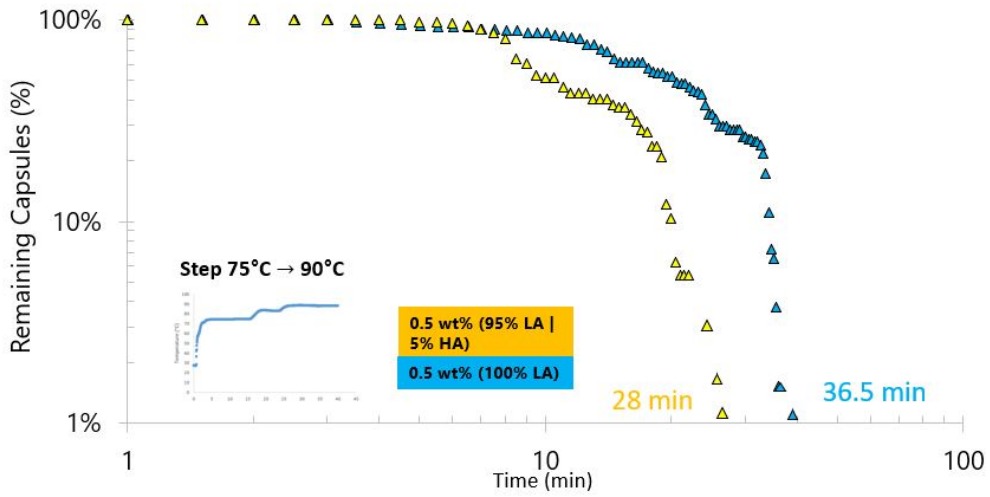

Figure 4.25: Evolution of microcapsule degradation under the heat rate increase protocol for shells with (D=450.3 μm, t/D=7.7%).

Analyzing the release behavior, in figure 4.25, for the capsules with an intermediate thickness-diameter ratio (D=450.3 μm, t/D=7.7%) we can see that:

- As with the previous t/D system, the capsules continued to indicate to be more trigger sensitive.;
- The total time required for its full release was 28 minutes;

Once again we see that the shell thickness influences the temperature response. Even with another type of gellan in its composition, the results show a tendency to increase the test time as there is more gellan percentage in the microcapsule, but as we include a concentration of acetylated gellan (high-acyl) in the composition of the shell, the overall test time is reduced compared to deacetylated (low-acyl) gellan. So far the preliminary structure tests we performed earlier, showing the high-acyl weakness, supports the results so far, as they respond faster to the trigger.

Although we made tests for the thickest capsules of table 4.6 (D=463.4 μm, t/D=9.1%), technical problems made the reliability of the results unfeasible. Therefore, the results obtained will not be showed or compared in this text.

4.3 Conclusions

Gellan-based microcapsules are temperature sensitive if inserted in a medium prone to activation of the thermal trigger. The degradation time depends on the physical and chemical properties of the substance.

The results presented in this chapter show the complete degradation of the samples inserted in a sodium acetate buffer (pH=4.5) in the properly sealed kline plate. The internal phase of the particle is composed of filtered sunflower oil and gellan makes up the shell wall of the capsule. The response was analyzed at different temperature levels to find an optimal test temperature. The results show that physical characteristics changed the release dynamics. Microcapsules with larger size and thickness-diameter ratios require more time to deliver all the encapsulated content.

To accelerate the release, the heat rate increase protocol was implemented. The behavior during testing was similar. However, the testing time has been greatly reduced. The percentage of time reduction increased as the shell thickness increased. Higher amounts of gellan in the shell were shown to be more sensitive to the temperature trigger.

In addition, we have also explored the effect of the gellan gum composition in the shell. We added to the mix a chain of natural high-acyl gellan, which is structurally weaker but with elastic characteristics. The results showed that this new gellan is more sensitive to the temperature trigger leading to shorter release time for the same temperature step.

5
Final remarks and suggestions

This dissertation aimed to experimentally investigate the behavior of gellan-based microcapsules under the influence of a thermal trigger event.

The gellan-gum capsules were produced by one-step double emulsion template process using microfluidics techniques. Physical parameters of the drops produced are directly linked to the geometry to which the fluids flow and to the flow rates of the internal, intermediate, and external phases. In addition to reproducing the geometry of the study of Michelon et al. [3], we developed a second device capable of generating larger microcapsules. Thus, we were able to produce microcapsules with different diameters and shell thickness in order to investigate the effect of these parameters on the release dynamics. The diameter and shell thickness of the microcapsules are key parameters that define the release time, as the amount of gellan in the shell affects its response to the temperature trigger event.

An operability window was mapped to evaluate at which flow rates the best production regime - dripping - can be achieved. This evaluation showed that the window of success is short. Two types of gellan-gum were used as shell material: one with pure low-acyl (LA) form and another with mixture a low-acyl and high-acyl (HA) form. Despite being crafted to have the same physical properties, they had different operability windows in the microfluidic production due to their chemical composition.

To carry out the controlled release testes it was necessary to build an experimental bath capable of withstanding high temperatures and being translucent enough so that the capsules could be viewed in real-time. The kick-off to identify at which temperatures the gellan-based shell reacts was through the fixed temperature protocol for both pure LA and mixtured LA-HA solutions. The triggers started around 70°C and, from then on, the ideal level for the controlled release of gellan actives was evaluated under constant temperature and we established that 75°C was the optimal temperature to guarantee the delivery of all gellan microcapsules inner content in a relative short time. Then, the physical properties of the capsules separated by groups of diameters and thickness were compared, under fixed temperature protocol and step increase on temperature protocol. The capsules from the small system

(D$<$ 250 μm) reacted to temperature with similar release times within the "small" groups. However, the large microcapsules group ($400 <$ D < 520 μm) capsules presented time for delivery of their actives much larger depending strongly on the amount of gellan presented in the capsule. Still, with the large capsule samples, we showed that increasing the environment temperature also increases the speed of delivery. However, the maximum working temperature value was 90 °C, due to water evaporation problems. Another interesting fact about the temperature rise protocol is evidence of the increase in delivery speed when the thickness increases, compared to the fixed temperature protocol.

We also tested the gellan microcapsules with high-acyl addition to the polymer chain. The results show that this addition of weaker molecules (HA) to the gellan polymer chain increases the reaction sensitivity to environment temperature. Release with altered gellan shell was faster than gellan with its LA form alone.

This work showed that gellan-based microcapsules can be used to controlled release of their inner content by a temperature change trigger. The time of delivery can be controlled by the geometry of the capsules and material used in the shell.

To continue this research in future works, some suggestions may be considered as studying higher percentages of the HA of gellan chain in the microcapsules shell in order to finding out how it can influence degradation. In addition, an improvement in the visualization field with fluorescent beads in the internal phase would be suitable to estimate the leakage during heat exchange. Another suggestion is to change the medium in which the microcapsules are inserted, preliminary tests with sunflower oil and pure water were not reactive to the test, so understanding the chemical interaction involved is essential to improve and facilitate the gellan release mechanisms. In addition, increasing the temperature, changing the heating method, changing the bath, try another hibrid systems with different resistances are also alternatives for future works.

Bibliography

[1] ESSER-KAHN, A. P.; ODOM, S. A.; SOTTOS, N. R.; WHITE, S. R. ; MOORE, J. S.. **Triggered release from polymer capsules**. Macromolecules, 44(14):5539–5553, 2011.

[2] UTADA, A. S.; LORENCEAU, E.; LINK, D. R.; KAPLAN, P. D.; STONE, H. A. ; WEITZ, D.. **Monodisperse double emulsions generated from a microcapillary device**. Science, 308(5721):537–541, 2005.

[3] MICHELON, M.; LEOPÉRCIO, B. C. ; CARVALHO, M. S.. **Microfluidic production of aqueous suspensions of gellan-based microcapsules containing hydrophobic compounds**. Chemical Engineering Science, 211:115314, 2020.

[4] MAO, R.; TANG, J. ; SWANSON, B.. **Texture properties of high and low acyl mixed gellan gels**. Carbohydrate polymers, 41(4):331–338, 2000.

[5] OSMAŁEK, T.; FROELICH, A. ; TASAREK, S.. **Application of gellan gum in pharmacy and medicine**. International journal of pharmaceutics, 466(1-2):328–340, 2014.

[6] ABBASPOURRAD, A.; DATTA, S. S. ; WEITZ, D. A.. **Controlling release from ph-responsive microcapsules**. Langmuir, 29(41):12697–12702, 2013.

[7] LEOPÉRCIO, B. C.. **Gellan-based microcapsules: production and applications**. PhD thesis, PUC-Rio, 2021.

[8] SUN, B. J.; SHUM, H. C.; HOLTZE, C. ; WEITZ, D. A.. **Microfluidic melt emulsification for encapsulation and release of actives**. ACS applied materials & interfaces, 2(12):3411–3416, 2010.

[9] AMSTAD, E.; KIM, S.-H. ; WEITZ, D. A.. **Photo-and thermoresponsive polymersomes for triggered release**. Angewandte Chemie International Edition, 51(50):12499–12503, 2012.

[10] DATTA, S. S.; ABBASPOURRAD, A.; AMSTAD, E.; FAN, J.; KIM, S.-H.; ROMANOWSKY, M.; SHUM, H. C.; SUN, B.; UTADA, A. S.; WINDBERGS, M. ; OTHERS. **25th anniversary article: Double emulsion templated solid microcapsules: Mechanics and controlled release**. Advanced Materials, 26(14):2205–2218, 2014.

[11] AMSTAD, E.. **Capsules: their past and opportunities for their future**, 2017.

[12] XU, S.; TABAKOVIĆ, A.; LIU, X. ; SCHLANGEN, E.. **Calcium alginate capsules encapsulating rejuvenator as healing system for asphalt mastic**. Construction and Building Materials, 169:379–387, 2018.

[13] ABBASPOURRAD, A.; CARROLL, N. J.; KIM, S.-H. ; WEITZ, D. A.. **Polymer microcapsules with programmable active release**. Journal of the American Chemical Society, 135(20):7744–7750, 2013.

[14] DUBEY, R.. **Microencapsulation technology and applications**. Defence Science Journal, 59(1):82, 2009.

[15] NABAVI, S. A.; VLADISAVLJEVIĆ, G. T.; BANDULASENA, M. V.; ARJMANDI-TASH, O. ; MANOVIĆ, V.. **Prediction and control of drop formation modes in microfluidic generation of double emulsions by single-step emulsification**. Journal of colloid and interface science, 505:315–324, 2017.

[16] CHEN, P. W.; ERB, R. M. ; STUDART, A. R.. **Designer polymer-based microcapsules made using microfluidics**. Langmuir, 28(1):144–152, 2012.

[17] ZHAO, Y.; SHUM, H. C.; ADAMS, L. L.; SUN, B.; HOLTZE, C.; GU, Z. ; WEITZ, D. A.. **Enhanced encapsulation of actives in self-sealing microcapsules by precipitation in capsule shells**. Langmuir, 27(23):13988–13991, 2011.

[18] PENTELA, N.; RAINU, S.; DURAIPANDY, N.; BOOPATHI, A.; KIRAN, M.; SAMPATH, S. ; SAMANTA, D.. **Microcapsules responsive to ph and temperature: synthesis, encapsulation and release study**. SN Applied Sciences, 1(5):1–10, 2019.

[19] BAKRY, A. M.; ABBAS, S.; ALI, B.; MAJEED, H.; ABOUELWAFA, M. Y.; MOUSA, A. ; LIANG, L.. **Microencapsulation of oils: A comprehensive review of benefits, techniques, and applications**. Comprehensive reviews in food science and food safety, 15(1):143–182, 2016.

[20] WINDBERGS, M.; ZHAO, Y.; HEYMAN, J. ; WEITZ, D. A.. **Biodegradable core–shell carriers for simultaneous encapsulation of synergistic actives**. Journal of the American Chemical Society, 135(21):7933–7937, 2013.

[21] ZHANG, W.; ABBASPOURRAD, A.; CHEN, D.; CAMPBELL, E.; ZHAO, H.; LI, Y.; LI, Q. ; WEITZ, D. A.. **Osmotic pressure triggered rapid release of encapsulated enzymes with enhanced activity**. Advanced Functional Materials, 27(29):1700975, 2017.

[22] ZHANG, W.; QU, L.; PEI, H.; QIN, Z.; DIDIER, J.; WU, Z.; BOBE, F.; INGBER, D. E. ; WEITZ, D. A.. **Controllable fabrication of inhomogeneous microcapsules for triggered release by osmotic pressure**. Small, 15(42):1903087, 2019.

[23] LIU, L.; WU, F.; JU, X.-J.; XIE, R.; WANG, W.; NIU, C. H. ; CHU, L.-Y.. **Preparation of monodisperse calcium alginate microcapsules via internal gelation in microfluidic-generated double emulsions**. Journal of colloid and interface science, 404:85–90, 2013.

[24] LISERRE, A. M.; RÉ, M. I. ; FRANCO, B. D.. **Microencapsulation of bifidobacterium animalis subsp. lactis in modified alginate-chitosan beads and evaluation of survival in simulated gastrointestinal conditions**. Food Biotechnology, 21(1):1–16, 2007.

[25] MARTINS, E.; PONCELET, D. ; RENARD, D.. **A novel method of oil encapsulation in core-shell alginate microcapsules by dispersion-inverse gelation technique**. Reactive and Functional Polymers, 114:49–57, 2017.

[26] ROSAS-FLORES, W.; RAMOS-RAMÍREZ, E. G. ; SALAZAR-MONTOYA, J. A.. **Microencapsulation of lactobacillus helveticus and lactobacillus delbrueckii using alginate and gellan gum**. Carbohydrate polymers, 98(1):1011–1017, 2013.

[27] FANG, Z.; BHANDARI, B.. **Encapsulation of polyphenols–a review**. Trends in Food Science & Technology, 21(10):510–523, 2010.

[28] GHARSALLAOUI, A.; ROUDAUT, G.; CHAMBIN, O.; VOILLEY, A. ; SAUREL, R.. **Applications of spray-drying in microencapsulation of food ingredients: An overview**. Food research international, 40(9):1107–1121, 2007.

[29] RAYBAUDI-MASSILIA, R. M.; MOSQUEDA-MELGAR, J.. **Polysaccharides as carriers and protectors of additives and bioactive compounds in foods**. The complex word of polysacharides. Editorial InTech, Rijeka, Croacia. Cap, 16:429–53, 2012.

[30] WAZARKAR, K.; PATIL, D.; RANE, A.; BALGUDE, D.; KATHALEWAR, M. ; SABNIS, A.. **Microencapsulation: an emerging technique in the modern coating industry**. RSC advances, 6(108):106964–106979, 2016.

[31] PAULO, F.; SANTOS, L.. **Design of experiments for microencapsulation applications: A review**. Materials Science and Engineering: C, 77:1327–1340, 2017.

[32] GREEN, B. K.; LOWELL, S.. **Pressure responsive record materials**, Jan. 10 1956. US Patent 2,730,457.

[33] CHENG, S.; YUEN, C.; KAN, C. W. ; CHEUK, K.. **Development of cosmetic textiles using microencapsulation technology**. Research Journal of Textile and Apparel, 2008.

[34] MARTINS, I. M.; BARREIRO, M. F.; COELHO, M. ; RODRIGUES, A. E.. **Microencapsulation of essential oils with biodegradable polymeric carriers for cosmetic applications**. Chemical Engineering Journal, 245:191–200, 2014.

[35] CARVALHO, I. T.; ESTEVINHO, B. N. ; SANTOS, L.. **Application of microencapsulated essential oils in cosmetic and personal healthcare products–a review**. International journal of cosmetic science, 38(2):109–119, 2016.

[36] CHANG, T. M. S.. **Therapeutic applications of polymeric artificial cells**. Nature Reviews Drug Discovery, 4(3):221–235, 2005.

[37] ULUDAG, H.; DE VOS, P. ; TRESCO, P. A.. **Technology of mammalian cell encapsulation**. Advanced drug delivery reviews, 42(1-2):29–64, 2000.

[38] HUNT, N. C.; GROVER, L. M.. **Cell encapsulation using biopolymer gels for regenerative medicine**. Biotechnology letters, 32(6):733–742, 2010.

[39] ORIVE, G.; HERNANDEZ, R. M.; GASCON, A. R.; CALAFIORE, R.; CHANG, T. M.; DE VOS, P.; HORTELANO, G.; HUNKELER, D.; LACIK,

I.; SHAPIRO, A. J. ; OTHERS. **Cell encapsulation: promise and progress**. Nature medicine, 9(1):104–107, 2003.

[40] SCHROOYEN, P. M.; VAN DER MEER, R. ; DE KRUIF, C.. **Microencapsulation: its application in nutrition**. Proceedings of the Nutrition Society, 60(4):475–479, 2001.

[41] MADENE, A.; JACQUOT, M.; SCHER, J. ; DESOBRY, S.. **Flavour encapsulation and controlled release–a review**. International journal of food science & technology, 41(1):1–21, 2006.

[42] SINGH, M.; HEMANT, K.; RAM, M. ; SHIVAKUMAR, H.. **Microencapsulation: A promising technique for controlled drug delivery**. Research in pharmaceutical sciences, 5(2):65, 2010.

[43] PEANPARKDEE, M.; IWAMOTO, S. ; YAMAUCHI, R.. **Microencapsulation: a review of applications in the food and pharmaceutical industries**. Reviews in Agricultural Science, 4:56–65, 2016.

[44] LAM, P.; GAMBARI, R.. **Advanced progress of microencapsulation technologies: in vivo and in vitro models for studying oral and transdermal drug deliveries**. Journal of Controlled Release, 178:25–45, 2014.

[45] LI, J.; YANG, S.; MUHAMMAD, Y.; SAHIBZADA, M.; ZHU, Z.; LIU, T. ; LIAO, S.. **Fabrication and application of polyurea formaldehyde-bioasphalt microcapsules as a secondary modifier for the preparation of high self-healing rate sbs modified asphalt**. Construction and Building Materials, 246:118452, 2020.

[46] ZHANG, L.; ABBASPOURRAD, A.; PARSA, S.; TANG, J.; CASSIOLA, F.; ZHANG, M.; TIAN, S.; DAI, C.; XIAO, L. ; WEITZ, D. A.. **Core–shell nanohydrogels with programmable swelling for conformance control in porous media**. ACS Applied Materials & Interfaces, 12(30):34217–34225, 2020.

[47] MCCLEMENTS, D. J.; DECKER, E. A. ; WEISS, J.. **Emulsion-based delivery systems for lipophilic bioactive components**. Journal of food science, 72(8):R109–R124, 2007.

[48] MCCLEMENTS, D. J.. **Nanoparticle-and microparticle-based delivery systems: Encapsulation, protection and release of active compounds**. CRC press, 2019.

[49] KARAMBEIGI, M. S.; ABBASSI, R.; ROAYAEI, E. ; EMADI, M. A.. **Emulsion flooding for enhanced oil recovery: interactive optimization of phase behavior, microvisual and core-flood experiments**. Journal of Industrial and Engineering Chemistry, 29:382–391, 2015.

[50] KILPATRICK, P. K.. **Water-in-crude oil emulsion stabilization: review and unanswered questions**. Energy & Fuels, 26(7):4017–4026, 2012.

[51] DEHGHAN, A. A.; JADALY, A.; AYATOLLAHI, S. ; MASIHI, M.. **Acidic heavy oil recovery using a new formulated surfactant accompanying alkali–polymer in high salinity brines**. Journal of Surfactants and Detergents, 20(3):725–733, 2017.

[52] TADROS, T. F.. **Emulsion formation and stability**. John Wiley & Sons, 2013.

[53] CHEN, G.; TAO, D.. **An experimental study of stability of oil–water emulsion**. Fuel processing technology, 86(5):499–508, 2005.

[54] LOPETINSKY, R.. **Solids-stabilized emulsions: a review**. Colloidal particles at liquid interfaces, p. 186–224, 2006.

[55] TADROS, T. F.. **Emulsion science and technology: a general introduction**. Emulsion science and technology, 1:1–55, 2009.

[56] YANG, Y.; FANG, Z.; CHEN, X.; ZHANG, W.; XIE, Y.; CHEN, Y.; LIU, Z. ; YUAN, W.. **An overview of pickering emulsions: solid-particle materials, classification, morphology, and applications**. Frontiers in pharmacology, 8:287, 2017.

[57] IZMAILOVA, V.; YAMPOLSKAYA, G.. **Concentrated emulsions stabilized by macromolecules and the contributions of hans sonntag to this scientific field**. Colloids and Surfaces A: Physicochemical and Engineering Aspects, 142(2-3):125–134, 1998.

[58] BANCROFT, W. D.. **The theory of emulsification, vi**. The Journal of Physical Chemistry, 19(4):275–309, 2002.

[59] CLOWES, G.. **Protoplasmic equilibrium**. The Journal of Physical Chemistry, 20(5):407–451, 2002.

[60] BROWN, E. N.; KESSLER, M. R.; SOTTOS, N. R. ; WHITE, S. R.. **In situ poly (urea-formaldehyde) microencapsulation of dicyclopentadiene**. Journal of microencapsulation, 20(6):719–730, 2003.

[61] AKARTUNA, I.; STUDART, A. R.; TERVOORT, E.; GONZENBACH, U. T. ; GAUCKLER, L. J.. **Stabilization of oil-in-water emulsions by colloidal particles modified with short amphiphiles**. Langmuir, 24(14):7161–7168, 2008.

[62] AKARTUNA, I.; TERVOORT, E.; STUDART, A. R. ; GAUCKLER, L. J.. **General route for the assembly of functional inorganic capsules**. Langmuir, 25(21):12419–12424, 2009.

[63] DUAN, H.; WANG, D.; SOBAL, N. S.; GIERSIG, M.; KURTH, D. G. ; MÖHWALD, H.. **Magnetic colloidosomes derived from nanoparticle interfacial self-assembly**. Nano letters, 5(5):949–952, 2005.

[64] O'SULLIVAN, M.; ZHANG, Z. ; VINCENT, B.. **Silica-shell/oil-core microcapsules with controlled shell thickness and their breakage stress**. Langmuir, 25(14):7962–7966, 2009.

[65] CONVERY, N.; GADEGAARD, N.. **30 years of microfluidics**. Micro and Nano Engineering, 2:76–91, 2019.

[66] BEEBE, D. J.; MENSING, G. A. ; WALKER, G. M.. **Physics and applications of microfluidics in biology**. Annual review of biomedical engineering, 4(1):261–286, 2002.

[67] WHITESIDES, G. M.. **Microfabrication, microstructures and microsystems**.

[68] WHITESIDES, G. M.. **The origins and the future of microfluidics**. nature, 442(7101):368–373, 2006.

[69] ZHANG, J.-Y.; ZENG, L.-H. ; FENG, J.. **Dynamic covalent gels assembled from small molecules: from discrete gelators to dynamic covalent polymers**. Chinese Chemical Letters, 28(2):168–183, 2017.

[70] SAHA, D.; BHATTACHARYA, S.. **Hydrocolloids as thickening and gelling agents in food: a critical review**. Journal of food science and technology, 47(6):587–597, 2010.

[71] NAZIR, A.; ASGHAR, A. ; MAAN, A. A.. **Food gels: gelling process and new applications**. In: ADVANCES IN FOOD RHEOLOGY AND ITS APPLICATIONS, p. 335–353. Elsevier, 2017.

[72] HENNINK, W. E.; VAN NOSTRUM, C. F.. **Novel crosslinking methods to design hydrogels**. Advanced drug delivery reviews, 64:223–236, 2012.

[73] GOPONENKO, A. V.; DZENIS, Y. A.. **Role of mechanical factors in applications of stimuli-responsive polymer gels–status and prospects**. Polymer, 101:415–449, 2016.

[74] SCHIAVI, A.; CUCCARO, R. ; TROIA, A.. **Strain-rate and temperature dependent material properties of agar and gellan gum used in biomedical applications**. Journal of the mechanical behavior of biomedical materials, 53:119–130, 2016.

[75] ZIA, K. M.; TABASUM, S.; KHAN, M. F.; AKRAM, N.; AKHTER, N.; NOREEN, A. ; ZUBER, M.. **Recent trends on gellan gum blends with natural and synthetic polymers: A review**. International journal of biological macromolecules, 109:1068–1087, 2018.

[76] MORRIS, E. R.; NISHINARI, K. ; RINAUDO, M.. **Gelation of gellan–a review**. Food Hydrocolloids, 28(2):373–411, 2012.

[77] BACELAR, A. H.; SILVA-CORREIA, J.; OLIVEIRA, J. M. ; REIS, R. L.. **Recent progress in gellan gum hydrogels provided by functionalization strategies**. Journal of Materials Chemistry B, 4(37):6164–6174, 2016.

[78] TAYLOR, M. J.; TOMLINS, P. ; SAHOTA, T. S.. **Thermoresponsive gels**. Gels, 3(1):4, 2017.

[79] GRAHAM, S.; MARINA, P. F. ; BLENCOWE, A.. **Thermoresponsive polysaccharides and their thermoreversible physical hydrogel networks**. Carbohydrate polymers, 207:143–159, 2019.

[80] QUINN, F. X.; HATAKEYAMA, T.; YOSHIDA, H.; TAKAHASHI, M. ; HATAKEYAMA, H.. **The conformational properties of gellan gum hydrogels**. Polymer gels and networks, 1(2):93–114, 1993.

[81] KIRCHMAJER, D. M.; STEINHOFF, B.; WARREN, H.; CLARK, R. ; IN HET PANHUIS, M.. **Enhanced gelation properties of purified gellan gum**. Carbohydrate research, 388:125–129, 2014.

[82] OLIVEIRA, J. T.; MARTINS, L.; PICCIOCHI, R.; MALAFAYA, P.; SOUSA, R.; NEVES, N.; MANO, J. ; REIS, R.. **Gellan gum: a new biomaterial for cartilage tissue engineering applications**. Journal of Biomedical Materials Research Part A: An Official Journal of The Society for Biomaterials, The Japanese Society for Biomaterials, and The Australian Society for Biomaterials and the Korean Society for Biomaterials, 93(3):852–863, 2010.

[83] OGAWA, E.; MATSUZAWA, H. ; IWAHASHI, M.. **Conformational transition of gellan gum of sodium, lithium, and potassium types in aqueous solutions**. Food Hydrocolloids, 16(1):1–9, 2002.

[84] SMITH, A. M.; SHELTON, R. M.; PERRIE, Y. ; HARRIS, J. J.. **An initial evaluation of gellan gum as a material for tissue engineering applications**. Journal of biomaterials applications, 22(3):241–254, 2007.

[85] VIEIRA, S.; DA SILVA MORAIS, A.; GARET, E.; SILVA-CORREIA, J.; REIS, R. L.; GONZÁLEZ-FERNÁNDEZ, Á. ; OLIVEIRA, J. M.. **Self-mineralizing ca-enriched methacrylated gellan gum beads for bone tissue engineering**. Acta biomaterialia, 93:74–85, 2019.

[86] LAU, M.; TANG, J. ; PAULSON, A.. **Texture profile and turbidity of gellan/gelatin mixed gels**. Food Research International, 33(8):665–671, 2000.

[87] DO NASCIMENTO, D.; AVENDAÑO, J.; MEHLA, A.; MOURA, M.; CARVALHO, M. ; DUNCANSON, W.. **Flow of tunable elastic microcapsules through constrictions sci**, 2017.

[88] KIM, S.-H.; KIM, J. W.; CHO, J.-C. ; WEITZ, D. A.. **Double-emulsion drops with ultra-thin shells for capsule templates**. Lab on a Chip, 11(18):3162–3166, 2011.

[89] HWANG, J. R.; SEFTON, M. V.. **Effect of capsule diameter on the permeability to horseradish peroxidase of individual hema-mma microcapsules**. Journal of controlled release, 49(2-3):217–227, 1997.

[90] SING, C. E.; PERRY, S. L.. **Recent progress in the science of complex coacervation**. Soft Matter, 16(12):2885–2914, 2020.

[91] NAKASHIMA, T.; SHIMIZU, M. ; KUKIZAKI, M.. **Particle control of emulsion by membrane emulsification and its applications**. Advanced drug delivery reviews, 45(1):47–56, 2000.

[92] MARTINO, C.; BERGER, S.; WOOTTON, R. C. ; DEMELLO, A. J.. **A 3d-printed microcapillary assembly for facile double emulsion generation**. Lab on a Chip, 14(21):4178–4182, 2014.

[93] BARBIER, V.; TATOULIAN, M.; LI, H.; AREFI-KHONSARI, F.; AJDARI, A. ; TABELING, P.. **Stable modification of pdms surface properties by plasma polymerization: application to the formation of**

double emulsions in microfluidic systems. Langmuir, 22(12):5230–5232, 2006.

[94] THIELE, J.; ABATE, A. R.; SHUM, H. C.; BACHTLER, S.; FÖRSTER, S. ; WEITZ, D. A.. **Fabrication of polymersomes using double-emulsion templates in glass-coated stamped microfluidic devices**. Small, 6(16):1723–1727, 2010.

[95] GÓMEZ-MASCARAQUE, L. G.; SIPOLI, C. C.; DE LA TORRE, L. G. ; LÓPEZ-RUBIO, A.. **A step forward towards the design of a continuous process to produce hybrid liposome/protein microcapsules**. Journal of food engineering, 214:175–181, 2017.

[96] NISISAKO, T.; OKUSHIMA, S. ; TORII, T.. **Controlled formulation of monodisperse double emulsions in a multiple-phase microfluidic system**. Soft Matter, 1(1):23–27, 2005.

[97] SAN MIGUEL, A.; SCRIMGEOUR, J.; CURTIS, J. E. ; BEHRENS, S. H.. **Smart colloidosomes with a dissolution trigger**. Soft Matter, 6(14):3163–3166, 2010.

[98] DATTA, S. S.; ABBASPOURRAD, A. ; WEITZ, D. A.. **Expansion and rupture of charged microcapsules**. Materials Horizons, 1(1):92–95, 2014.

[99] JOKI, T.; MACHLUF, M.; ATALA, A.; ZHU, J.; SEYFRIED, N. T.; DUNN, I. F.; ABE, T.; CARROLL, R. S. ; BLACK, P. M.. **Continuous release of endostatin from microencapsulated engineered cells for tumor therapy**. Nature biotechnology, 19(1):35–39, 2001.

[100] PADSALGIKAR, A.. **Plastics in medical devices for cardiovascular applications**. William Andrew, 2017.

[101] LEE, H.; FISHER, S.; KALLOS, M. S. ; HUNTER, C. J.. **Optimizing gelling parameters of gellan gum for fibrocartilage tissue engineering**. Journal of Biomedical Materials Research Part B: Applied Biomaterials, 98(2):238–245, 2011.